A major purpose of the Technical Information Center is to provide the broadest dissemination possible of information contained in DOE's Research and Development Reports to business, industry, the academic community, and federal, state and local governments.

Although a small portion of this report is not reproducible, it is being made available to expedite the availability of information on the research discussed herein.

Los Alamos National Laboratory is operated by the University of California for the United States Department of Energy under contract W-7405-ENG-36.

TITLE MEASUREMENT OF GAS DENSITY AND TEMPERATURE PROFILES IN UF_6 USING LASER INDUCED FLUORESCENCE

LA-UR--85-2975

DE86 011473

AUTHOR(S) Stephen E. Caldwell
Richard A. Gentry
Ralph W. White
Steven W. Allison

SUBMITTED TO The Sixth Workshop on Gases in Strong Rotation
Tokyo, Japan

August 19-23, 1985

DISCLAIMER

Los Alamos Los Alamos National Laboratory
Los Alamos, New Mexico 87545

FORM NO. 836 R4
ST. NO. 2629 5/81

THE SIXTH WORKSHOP ON GASES IN STRONG ROTATION

Aug. 19–23. 1985
TOKYO. JAPAN

TITLE Measurement of Gas Density and Temperature Profiles in UF_6 using Laser Induced Fluorescence*

NAME Stephen E. Caldwell, Richard A. Gentry, and Ralph W. White, Los Alamos National Laboratory, Los Alamos, NM, USA; Steven W. Allison, Martin Marietta Energy Systems, Oak Ridge, TN, USA

ABSTRACT

Laser induced fluorescence (LIF) can be used to determine the pressure and temperature of an UF_6 gas sample. An external pulsed laser is used to excite the gas and a multichannel fiber optics system simultaneously collects fluorescence signals emanating from a number of points in the gas. The signals are digitized and presented to a minicomputer for data reduction. Both fluorescence intensity and lifetime are used to deduce temperature and pressure.

The LIF probe system is described. Analysis of the data is discussed, and representative results are presented.

*Based on work performed by Los Alamos National Laboratory under subcontract (PO 10K-13674V) to Martin Marietta Energy Systems, Inc., for the U.S. Department of Energy, and work performed at the Oak Ridge Gaseous Diffusion Plant, operated by Martin Marietta Energy Systems, Inc., for the U.S. Department of Energy under Contract DE-AC05-84OR21400.

INTRODUCTION

Laser induced fluorescence, both lifetime and intensity, can be used to uniquely determine the temperature and pressure of UF_6 gas. We have developed a system for extracting multi-channel laser induced fluorescence (LIF) data from an operating gas centrifuge. This work was first reported by Gentry at the 4th Workshop on Gases in Strong Rotation (1981). Since that time, the technique has been refined, automated, and extended to include pressure and temperature measurements simultaneously.

LASER INDUCED FLUORESCENCE IN UF_6

Laser induced fluorescence in UF_6 has been studied over a pressure and temperature range[1,2,3] of interest to the gas centrifuge community. Excitation takes place in a broadband which extends from 375 to 420 nm (see Fig. 1), peaking at 392 nm. Fluorescence is also broadband; extending from 400 to 455 nm, with a peak at 421 nm. The fluorescence spectrum is essentially independent of excitation wavelength[1,4] and pressure.[4]

In a collisionless gas, the fluorescence lifetime would be approximately 56 μs.[5] Molecular collisions quench the fluorescence, presumably by causing dissociation of the excited molecules. Since the molecular collision rate is dependent upon both number density and particle velocity, the fluorescence lifetime is dependent upon both pressure and temperature. This is shown in Fig. 2.

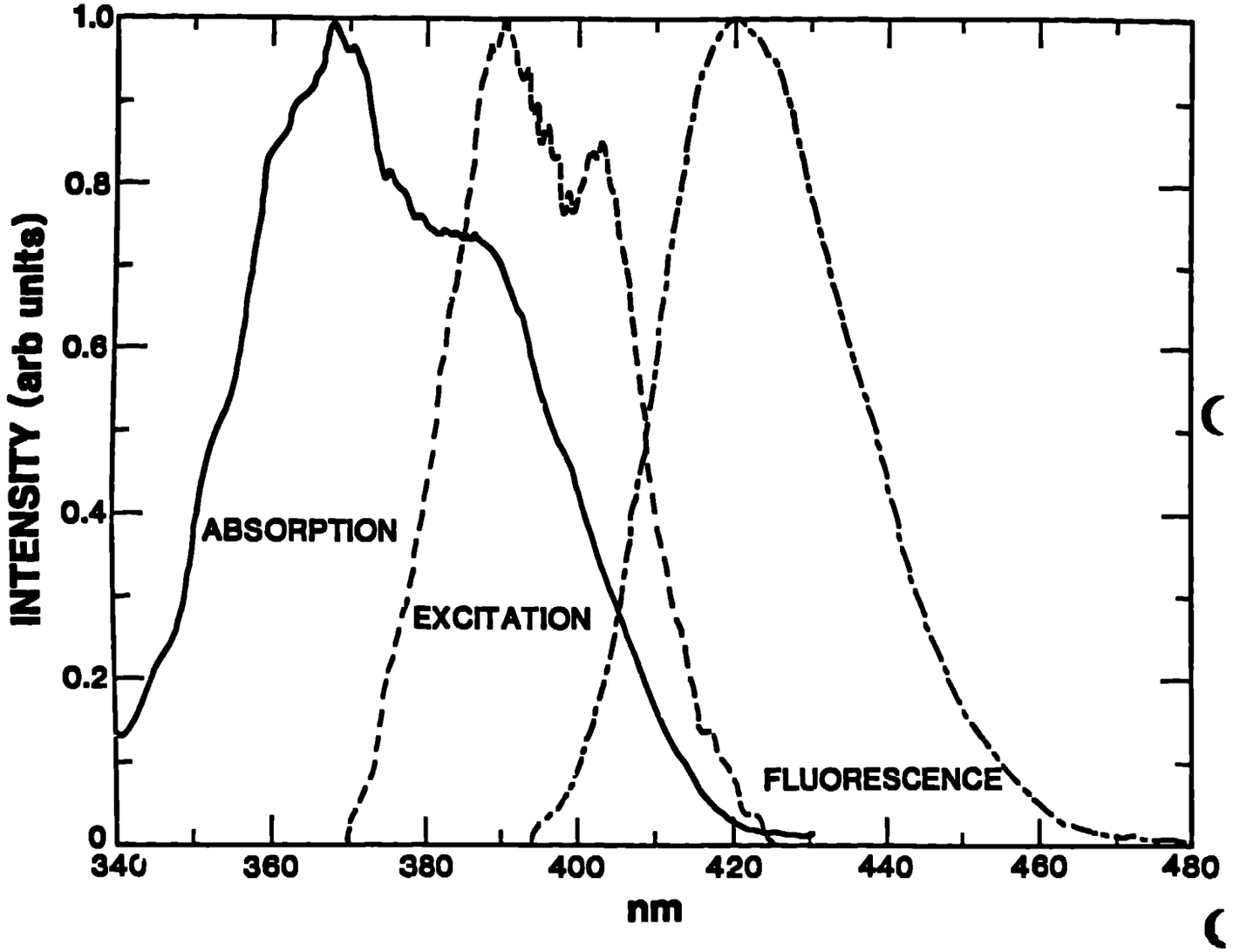

Fig. 1. UF_6 excitation and fluorescence spectra (from Ref. 4).

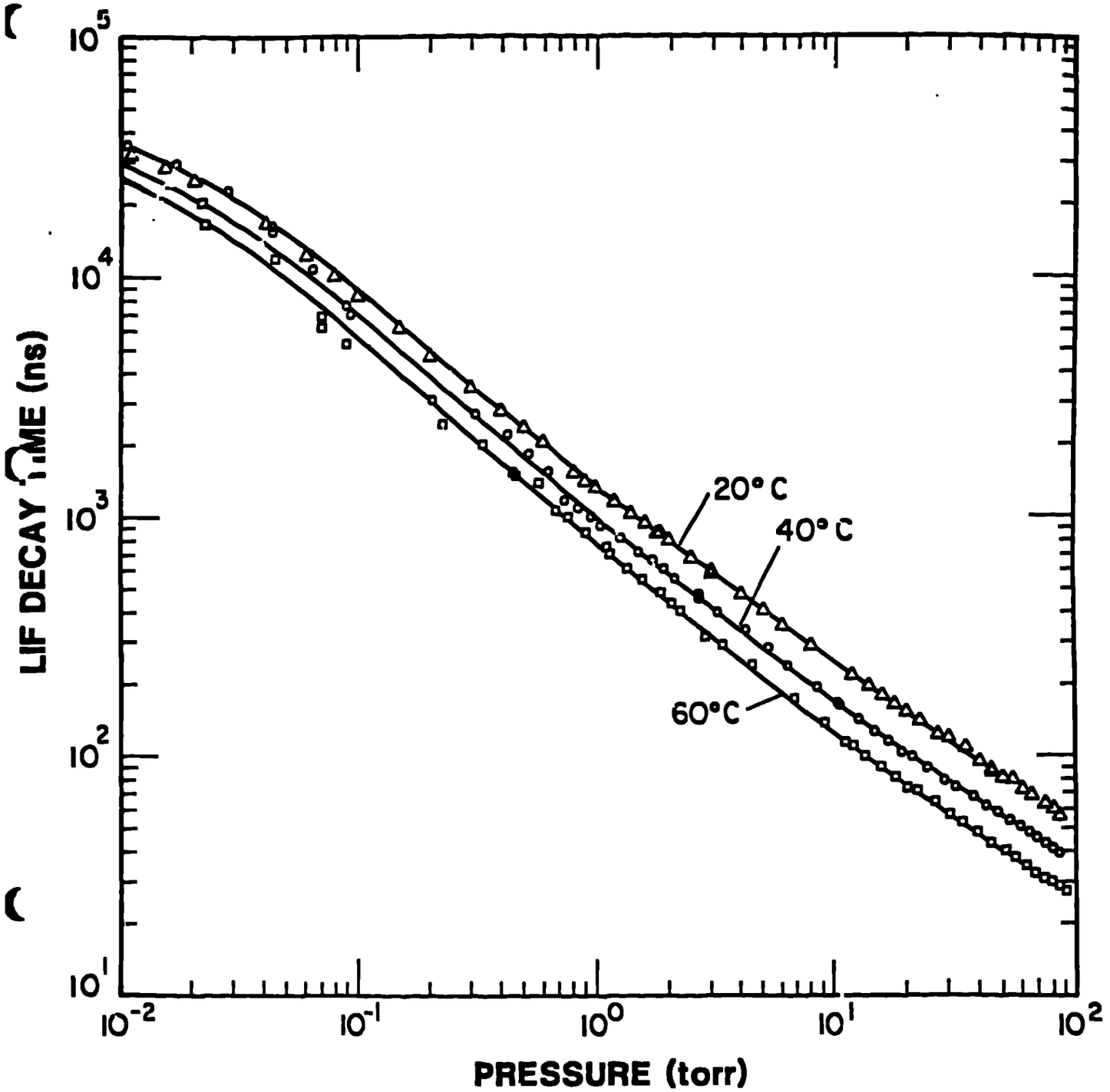

Fig. 2. UF_6 fluorescence lifetime is dependent upon both temperature and pressure.

Oldenborg, et al,[4,5] have developed a simple model, based on the level structure of Fig. 3, to explain the data of Fig. 2. This model leads to the following expression for the fluorescence lifetime (τ):

$$\frac{1}{\tau} = k_U + k_C P + k_1 P \frac{1 + (\alpha + \beta)P}{1 + (\alpha + \beta + \gamma)P + \beta\gamma P^2} \quad . \qquad (1)$$

P is pressure, and

k_U, k_C, k_1, α,β,γ are experimentally determined constants.

Each constant is assumed to satisfy an Arrhenius relationship of the form

$$k = Ae^{-E/RT} \qquad (2)$$

where E is the activation energy and R is the ideal gas constant. A least squares fit to the data (Fig. 2) yields the constants given in Table 1.[5]

TABLE 1

Arrhenius Parameters for UF_6 Self-Quenching Rate Constants at 392.1 nm

Rate Constant	A		E/R (K)
k_U	$(2.30 \pm 1.13)*10^5$	s^{-1}	761.6 ± 131.5
k_C	$(1.31 \pm 1.90)*10^8$	$torr^{-1}\ s^{-1}$	2114 ± 440
k_1	$(2.43 \pm 0.68)*10^7$	$torr^{-1}\ s^{-1}$	953.3 ± 85.1
α	60.0 ± 156	$torr^{-1}$	1693 ± 791
β	11.2 ± 19.3	$torr^{-1}$	1731 ± 517
γ	0.215 ± 0.401	$torr^{-1}$	-260.3 ± 557.9

Data Range: 0.005 - 85 torr
20 - 60°C (10° intervals)

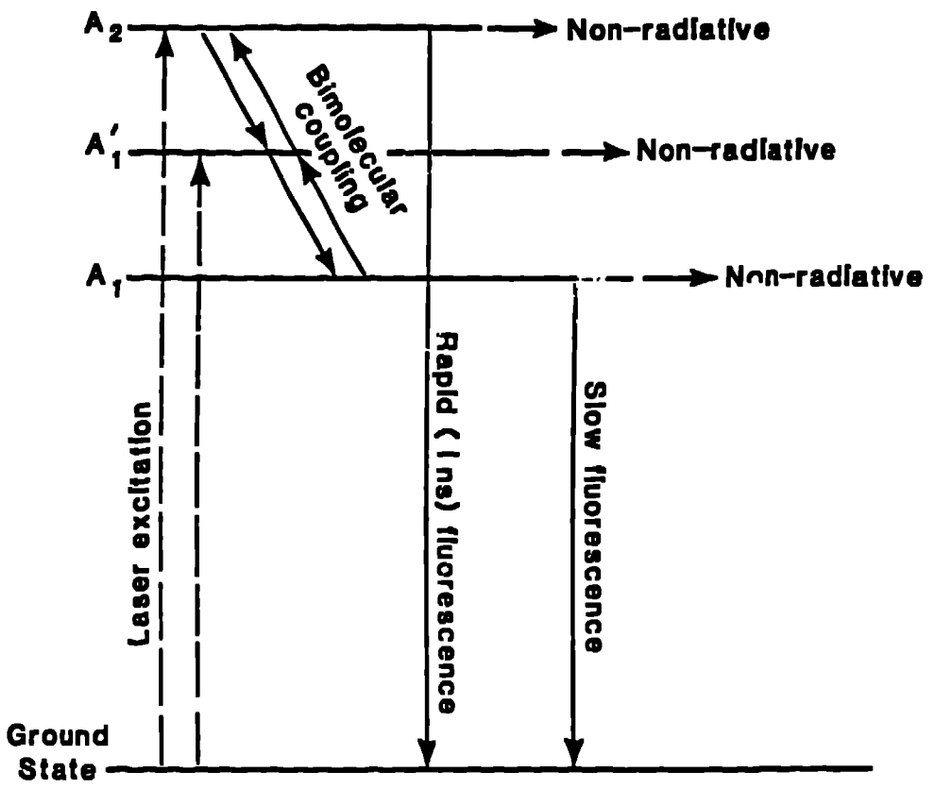

Fig. 3. Proposed excitation model for UF_6. This simple model is sufficient to explain the observed data. This work uses only the slow fluorescence. Rapid fluorescence has been reported by DeWitte et al.[2]

Fluorescence intensity is also dependent on both molecular number density and temperature. The fluorescence signal is of the form

$$Y = Ie^{-t/\tau} \quad , \tag{3}$$

where t = time
$\tau = \tau(n,T)$
$I = I(n,T)$
n = gas molecular number density
T = temperature

The intensity factor, $I(n,T)$, is directly proportional to the number of laser excited molecules which in turn is directly proportional to the molecular number density, n. The temperature dependence of $I(n,T)$ arises from the UF_6 photon cross section which has been measured by Wampler[6] et al:

$$\sigma = (1.312 + 0.012T - 8.5 * 10^{-5}T^2)10^{-20} \text{ cm}^2, \tag{4}$$
for $20 < T < 60$ T in ^oC,
and $\lambda = 392.1$ nm.

From the above discussion it can be seen that UF_6 gas pressure and temperature can be unfolded from measurements of laser induced fluorescence lifetime and intensity. The "measurability" of the pressure, P, and temperature, T, can be defined as the rate of change of the observed characteristic with respect to the rate of change of the desired parameter:

$$\begin{aligned} M(\tau,T) &= \frac{\Delta\tau/\tau}{\Delta T/T} = \frac{T}{\tau}\frac{\partial\tau}{\partial T} \\ M(\tau,P) &= \frac{\Delta\tau/\tau}{\Delta P/P} = \frac{P}{\tau}\frac{\partial\tau}{\partial P} \\ M(I,T) &= \frac{\Delta I/I}{\Delta T/T} = \frac{T}{I}\frac{\partial I}{\partial T} \\ M(I,P) &= \frac{\Delta I/I}{\Delta P/P} = \frac{P}{I}\frac{\partial I}{\partial P} \end{aligned} \tag{5}$$

$M(\tau,T)$ and $M(\tau,P)$ are determined from Eq. 1 and Table 1. These are plotted in Fig. 4. $M(I,T)$ is found using Eq. 4 and is plotted in Fig. 5. $M(I,P)$ is identically equal to 1.0 because both intensity and pressure are directly proportional to molecular number density.

A large measurability implies that the observed characteristic is very sensitive to small changes in the desired parameter. For example, $M(\tau,T) = 4$ implies that a 1% change in temperature will be observed as a 4% change in fluorescence lifetime. Likewise, a 4% measurement error of lifetime will be reflected as a 1% measurement error of temperature. A quick study of Figs. 4 and 5 would suggest that lifetime measurements be used to determine temperature and intensity measurements be used to determine pressure.

APPARATUS

Optics

The UF_6 gas to be sampled is located within a few centimeters of the wall of the centrifuge. A moderately high vacuum is maintained inside (smaller radius) the gas region. Figure 6 is a schematic of the STR bowl and LIF optics.

An externally produced 392.1 nm laser beam is directed into the gas layer near the rotor wall and the resulting fluorescence light is transmitted to photomultiplier tubes located outside the vacuum system. All hardware are positioned in the vacuum core, far from the rotor wall, in order to avoid disturbing the gas flow.

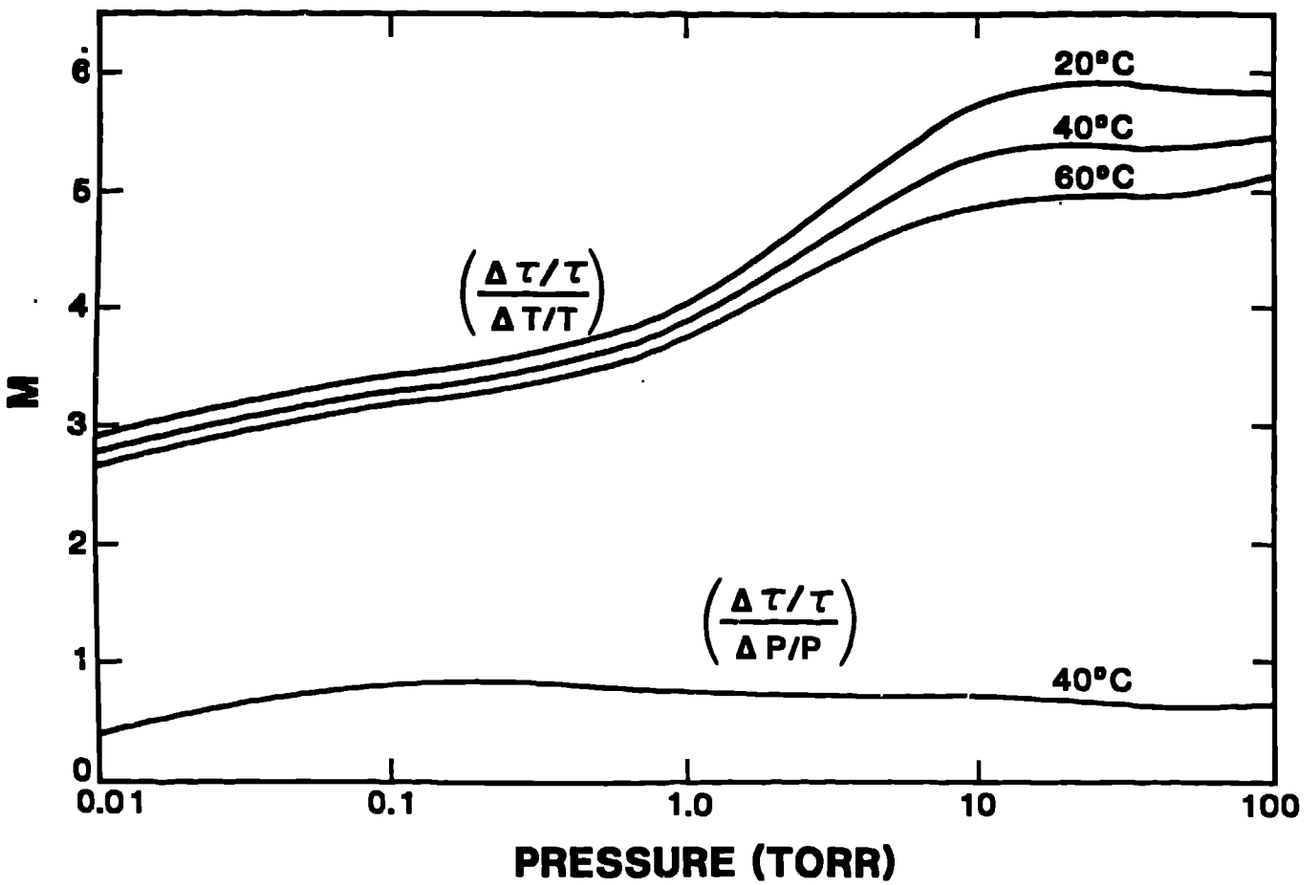

Fig. 4. $M(\tau,T)$ and $M(\tau,P)$. The measurability of temperature and pressure using fluorescence lifetime, τ. The temperature dependence of $M(\tau,P)$ cannot be distinguished on the scale of this plot.

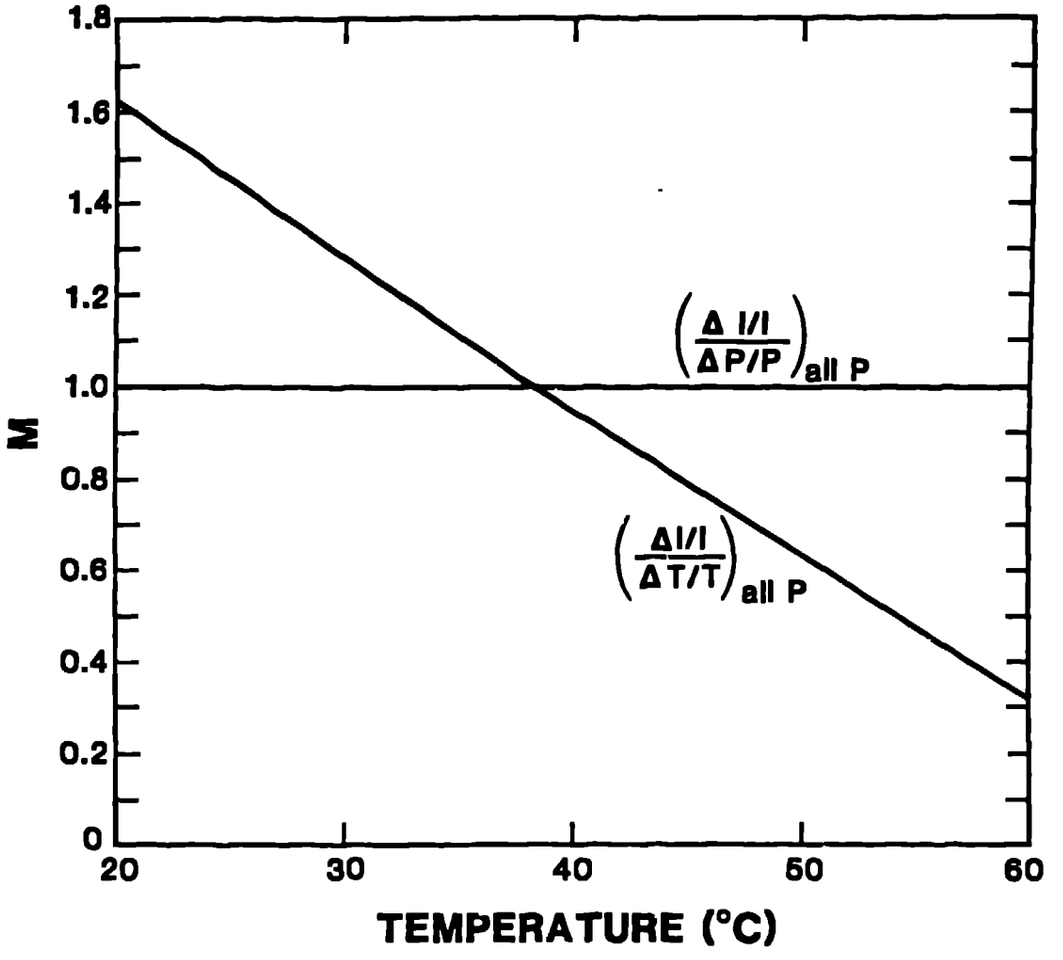

Fig. 5. M(I,T) and M(I,P). The measurability of temperature and pressure using fluorescence intensity, I.

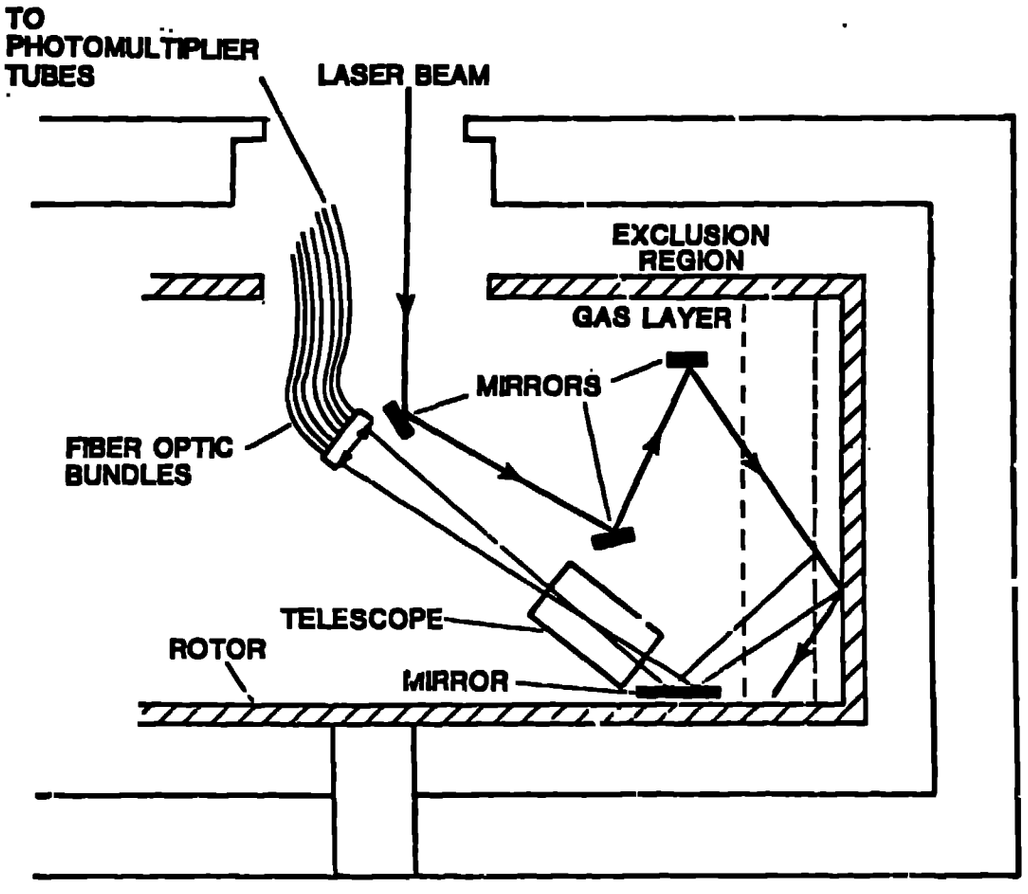

Fig. 6. Schematic diagram of internal optics.

Three internal mirrors direct the laser beam to intersect the wall at an angle of 55° to the normal. Excited UF_6 molecules form a line source of fluorescent light. A telescope produces an image of fluorescing gas on the face of a fiber optics bundle, located near the axis of the rotor. The telescope consists of two lenses (42 mm diameter x 150 mm focal length) and two broadband filters that pass the fluorescence band (400 - 440 nm) and reject scattered laser light (392.1 nm).

The fiber optics bundle dissects the fluorescence image into 26 parts (see Fig. 7), representing 26 radial locations of gas samples. The light from each of the 26 sub-images is carried via its own incoherent fiber bundle to an externally mounted photomultiplier tube. Figure 8 is a photograph of the optics internal to the centrifuge.

Electronics

Photomultiplier tubes convert the fluorescence into an electrical pulse. The analogue electrical signals are then digitized and presented to an LSI 11/2 minicomputer through the use of CAMAC based current integrators.

An oscilloscope trace of a typical LIF signal is shown in Fig. 9. The initial higher amplitude spike is caused by scattered light from the laser excitation pulse, which is far more intense than the fluorescence signal. The later, exponentially decaying portion of the trace is the actual fluorescence signal, visible after the laser has been extinguished. The fluctuations are caused mostly by photon statistics. In the illustration of

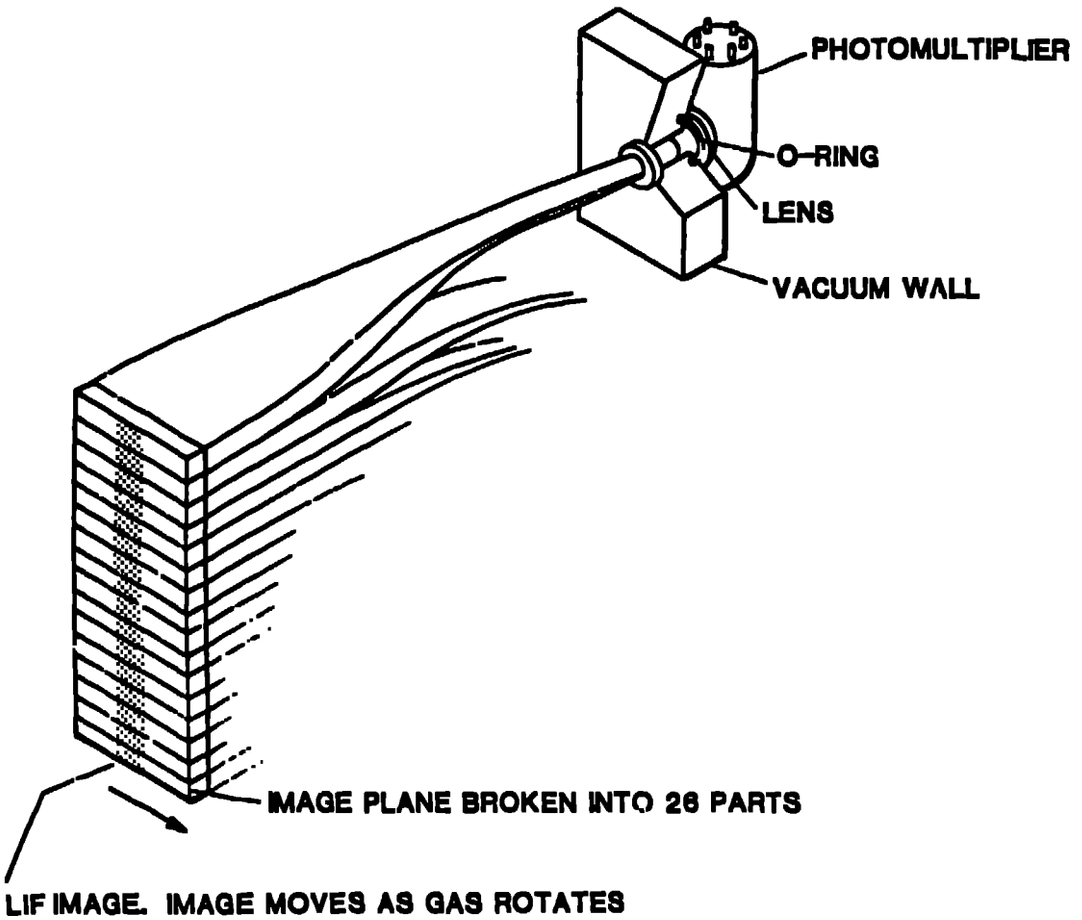

Fig. 7. The fiber optics bundle dissects the continuous LIF image into 26 discrete packets and carries the light to 26 photomultiplier tubes located outside the vacuum system.

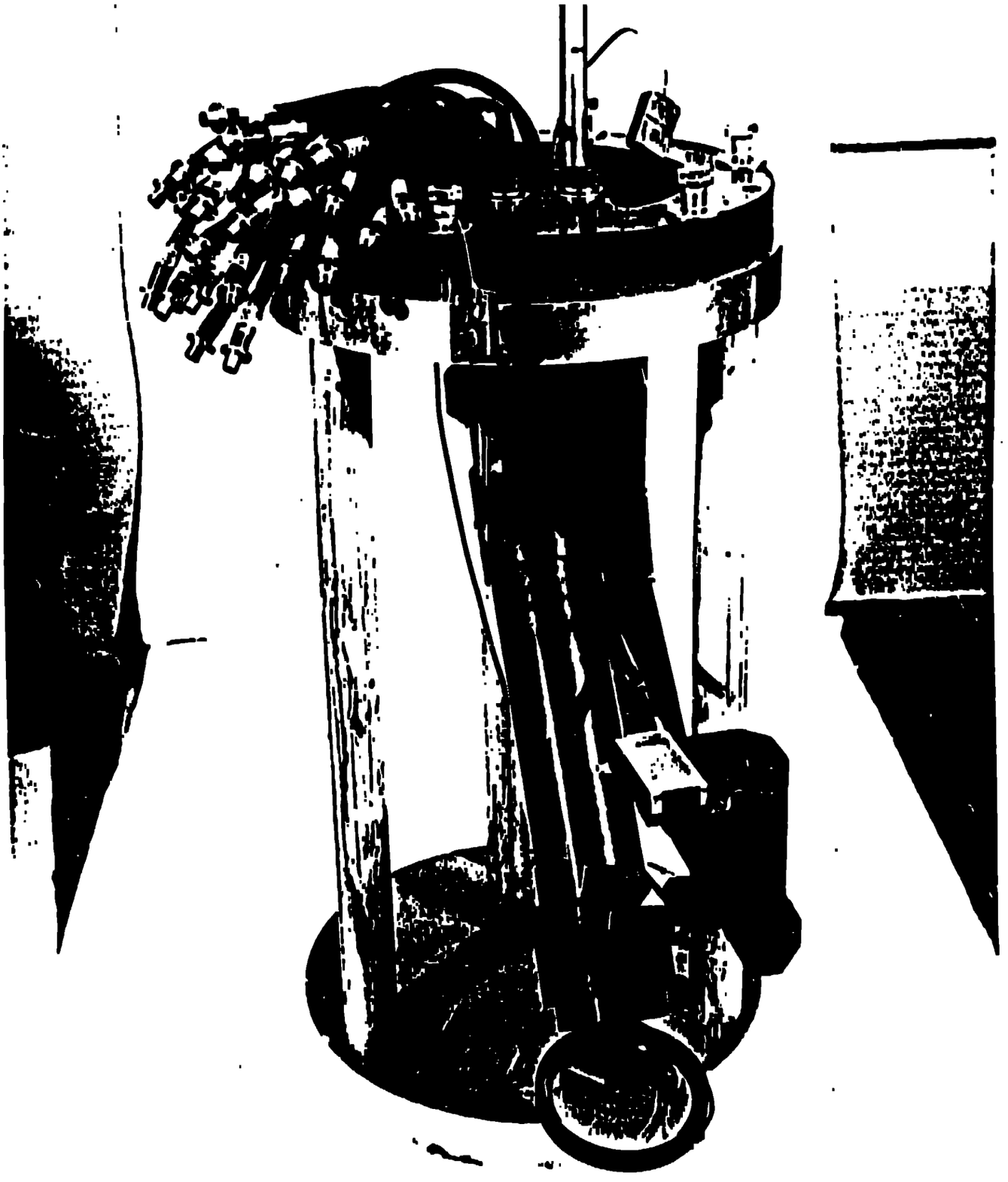

Fig. 8. Photograph of internal optics. The three rectangular mirrors direct the laser beam to the sample region. The round mirror collects the fluorescent light for the telescope which is contained in the black cylinder. Twenty-six fiber bundles, seen at the top, carry light to the vacuum wall. The aluminum stand does not go into the centrifuge.

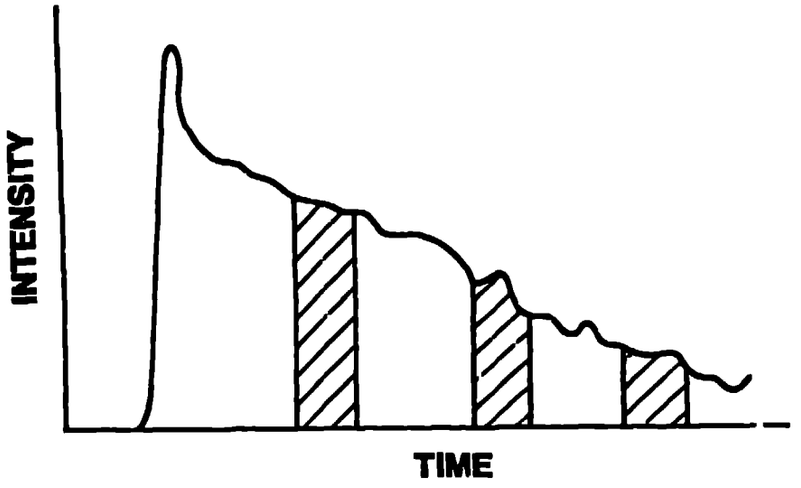

Fig. 9. LIF signal. The signal is traced from an oscilloscope photograph of LIF decay from a single laser pulse. The crosshatched areas demonstrate how current integrators can be used to sample the exponential signal.

Fig. 9, the gated current integrators sample portions of the curve. These samples can then be used in a least squares fit to determine fluorescence lifetime and intensity.

Figure 10 can be used to explain how multiple samples are taken of a single pulse. The analogue pulse is split into three identical pulses, using a matched signal divider, and presented to three current integrators. Each integrator is separately gated after a fixed delay from the laser pulse. The current integrators are CAMAC modules under the control of an LSI 11/2 minicomputer.

Figure 11 is a photograph of a matched fanout. Figure 12 is a photograph of a Delayed Gate Generator designed and built at Los Alamos. All other electronics are commercially available. The Delayed Gate Generators provide twenty gate pulses (front panel) per trigger (rear panel). The width of each gate is adjustable in ~ 6 ns intervals from 20 to 200 ns by means of wire wrap pins. Delays are sequential (output 2 is delayed longer than output 1, etc.) in steps of 5, 10, 20, 50, 70, 90, 100, or 200 ns as determined by the delay chips at the rear of the PC board. An output at the rear panel, which is delayed like output #20, can be used to trigger a second module. Twenty of these modules (400 available gates) are sufficient to simultaneously cover all 26 optical channels in any running configuration. Figure 13 is a photograph of the fanouts, Delayed Gate Generators, and current integrators mounted in a standard equipment rack.

System Integration

The entire system is shown schematically in Fig. 14. The laser beam enters the centrifuge through a quartz window in the

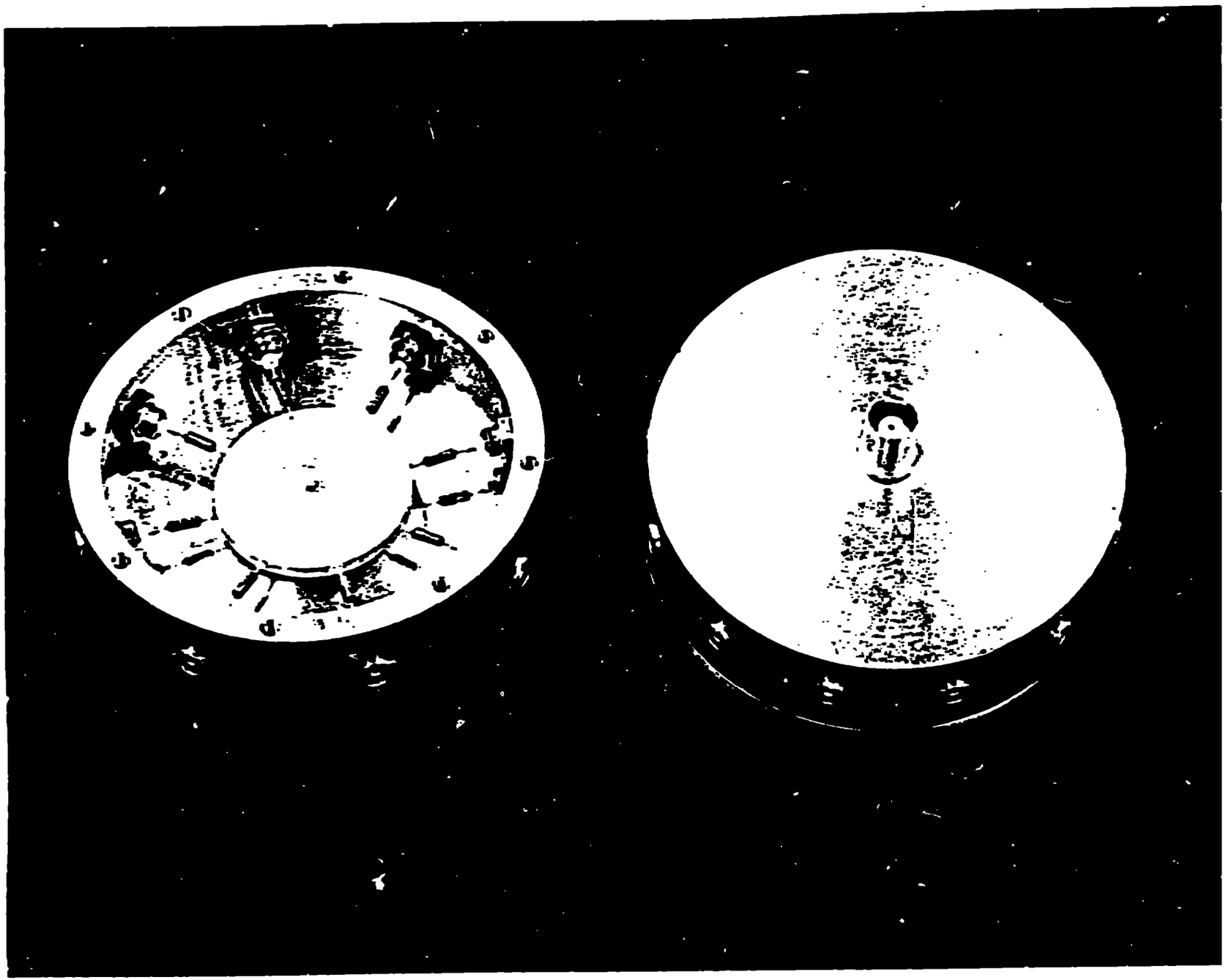

Fig. 11. Passive matched fanout.

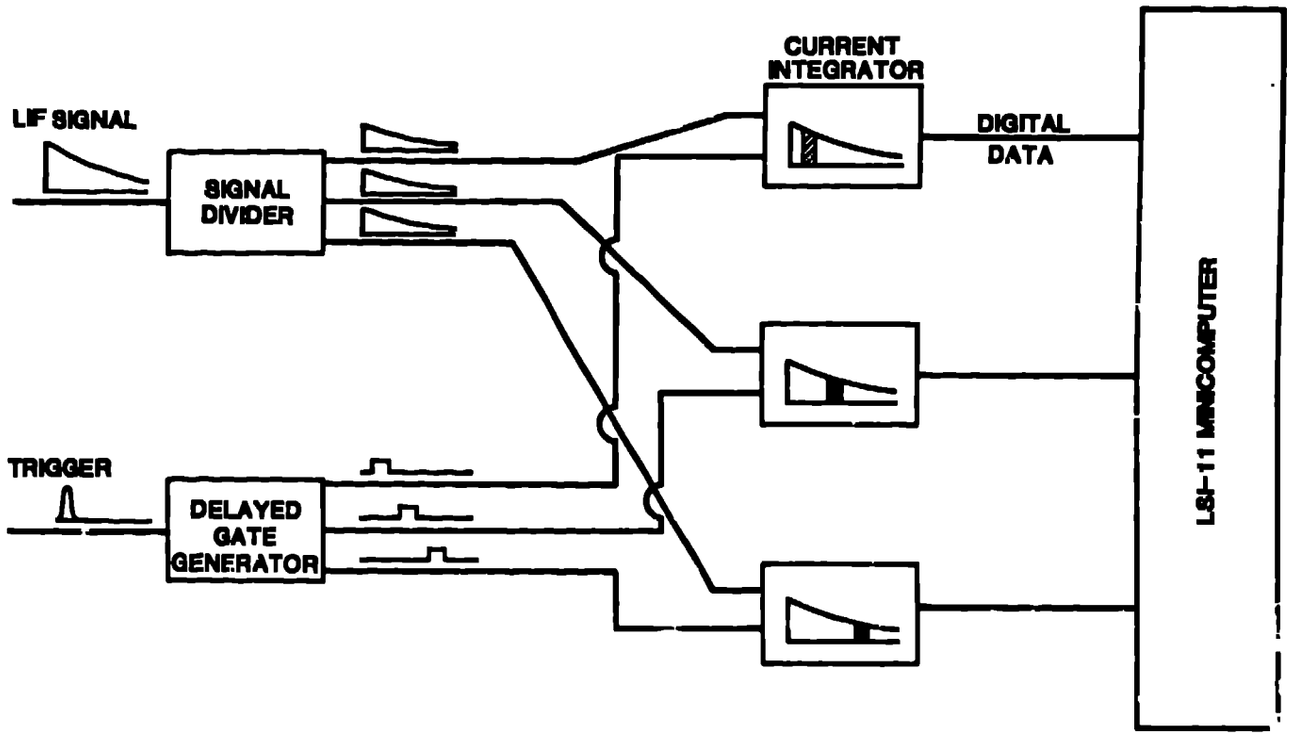

Fig. 10. Multiple sampling of a single pulse. In practice, about 10 samples are taken.

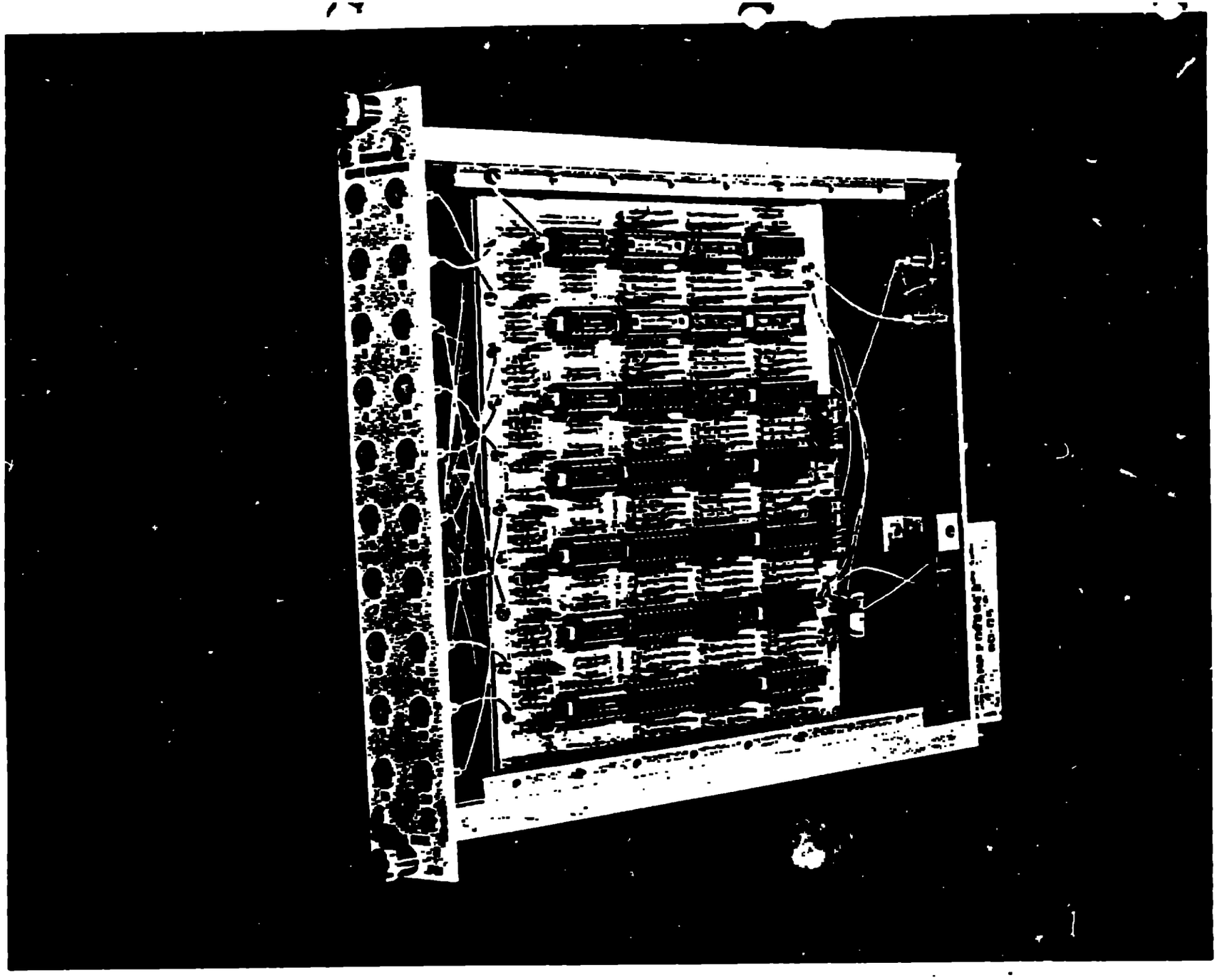

Fig. 12. Delayed Gate Generator.

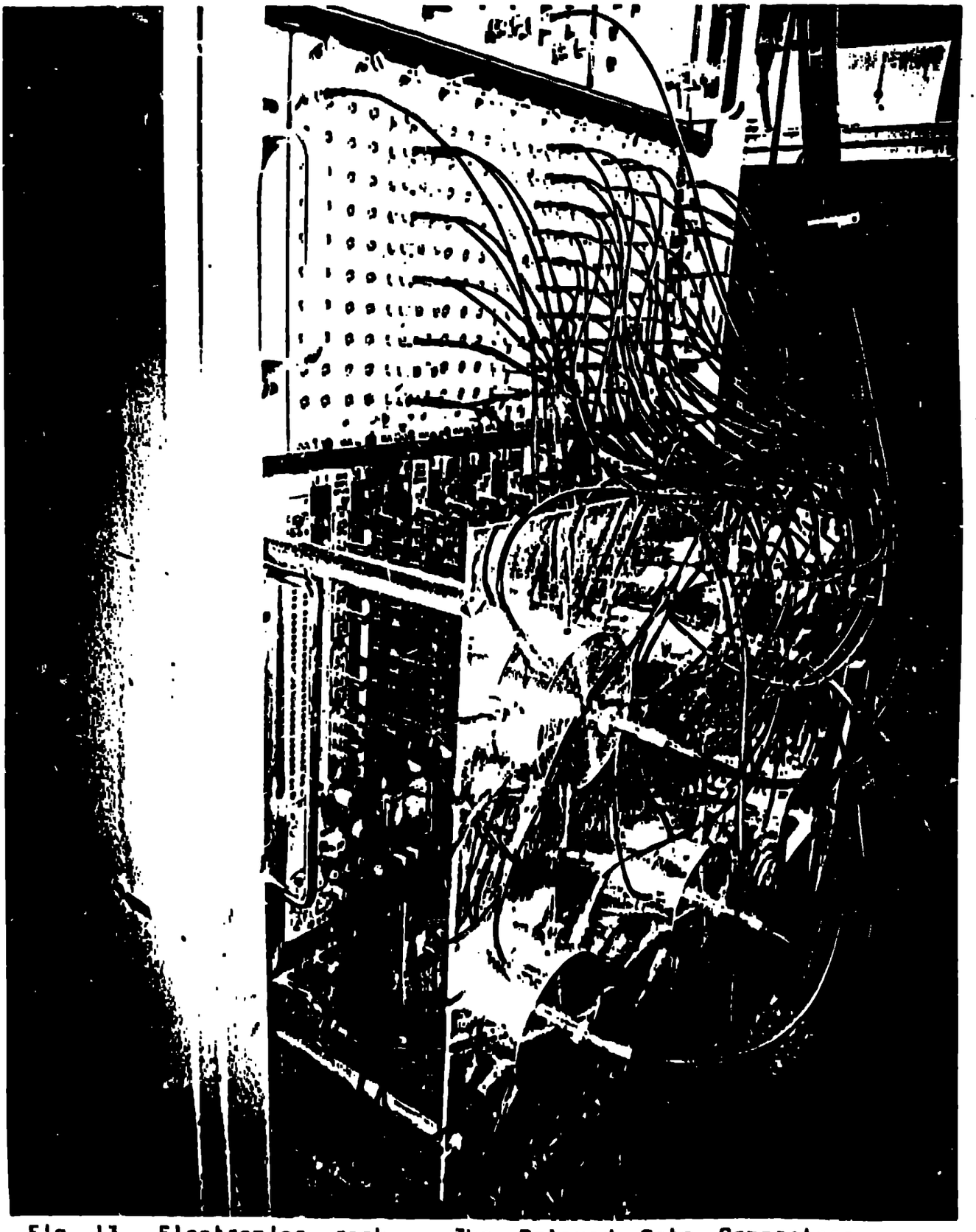

Fig. 13. Electronics rack. The Delayed Gate Generators are mounted in a NIM bin. The current integrators are located in the CAMAC crate behind the fanouts. All electronics needed to operate 26 optical channels (including computer) would occupy two equipment racks.

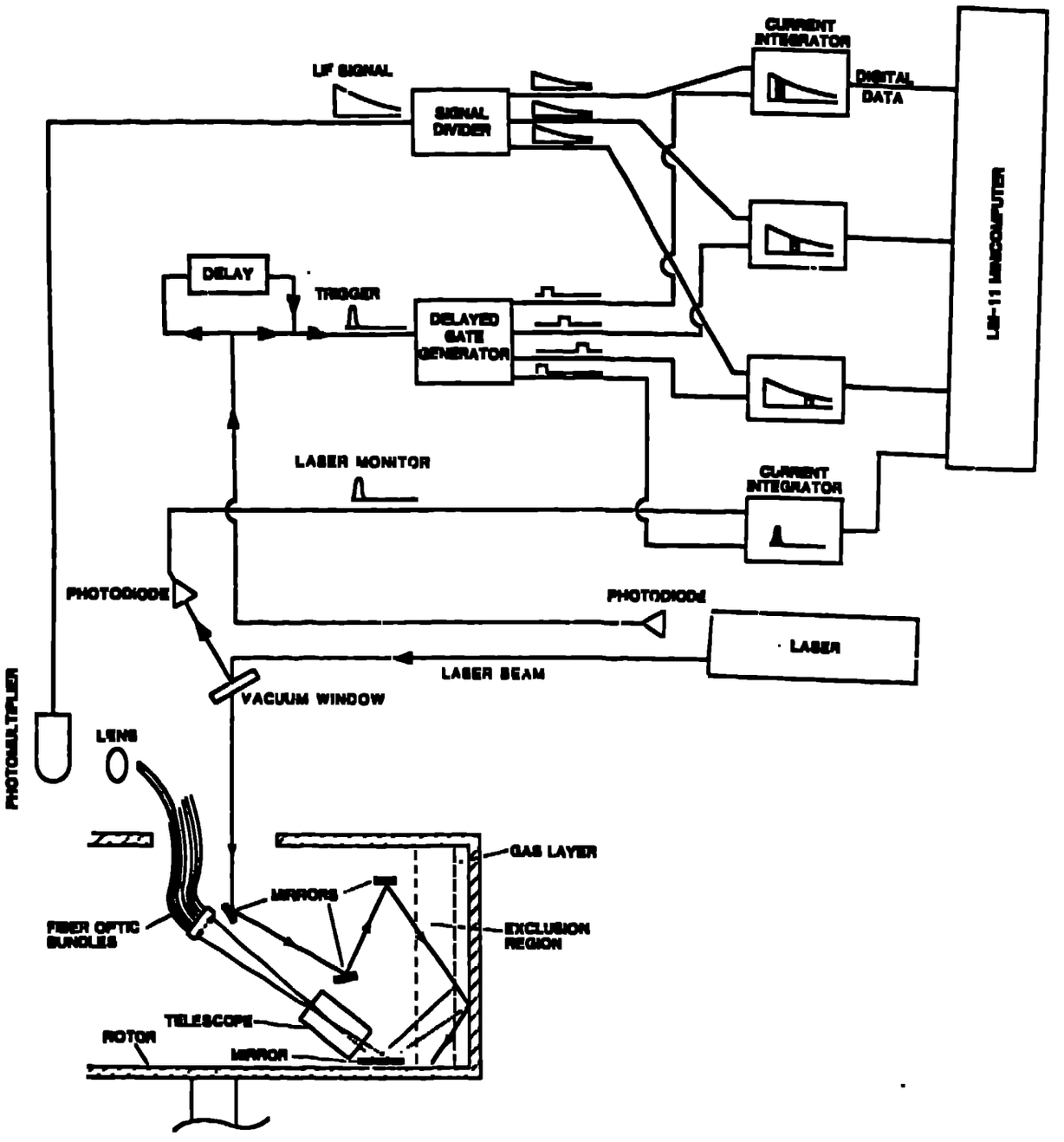

Fig. 14. System schematic.

vacuum chamber wall. This window is tilted so that the reflected laser pulse is seen by a photodiode. The photodiode signal, which is proportional to the laser pulse intensity, is recorded with a current integrator. Since the fluorescence intensity is directly proportional to laser pulse energy, this photodiode signal is used to normalize the measured fluorescence intensity.

A second photodiode, which looks at scattered light from the laser, is used to trigger the Delayed Gate Generators. The LSI-11/2 is notified, via the CAMAC interface, when the current integrators have recorded data. The computer requests/receives data from each integrator then resets the integrators in preparation for more data. Note that the photodiode also triggers a delay pulser which again triggers the Delayed Gate Generators after a pause of 40 ms. This allows background data to be recorded in all integrators. The background data is collected by the computer, subtracted from the real fluorescence data, and the result is normalized (divided by) to the laser monitor data.

To reduce the effects of photon statistics, multiple laser pulses (typically 100) are collected and summed at ~ 10 Hz rate. The collection of data over multiple laser shots allows the computer to determine mean and standard deviation values for each integrator.

At the end of each run, the computer does a least squares fit to the data from each detector, determining both fluorescence lifetime and intensity. The results and data are put into archival storage for later printout or plotting. Conversion of

the lifetime-intensity data into pressure-temperature information has not been automated.

Sampling

CAMAC housed current integrators are used to sample the photomultiplier output. The signal shape is known to be exponential, so the samples are used only to determine lifetime and intensity. A simple-minded statistical analysis was used to confirm the following intuitive features of sampling:

1) More samples are always better, but the incremental improvement decreases rapidly above ~ 8 samples.

2) Sampling should begin as early as possible and continue as long as practicable.

3) Sample intervals should be contiguous.

4) Sample widths should be adjusted so as to present equal charge to each integrator (i.e. late time gates should be wider than early time gates).

The current integrators cannot be used with gates wider than ~ 200 ns. The Delayed Gate Generators cannot produce a gate narrower than ~ 20 ns. Effectively narrower gates can be made by overlapping the samples. For example:

Gate 1	100 - 120 ns
Gate 2	110 - 130 ns
Gate 3	120 - 140 ns
etc.	

Other system considerations yield the following sampling constraints:

1) No sample should begin within 100 ns of the laser pulse. The reason for this is unknown, but samples taken before 100 ns usually appear high.

2) Samples should not be taken more than three lifetimes after the laser pulse. The finite gas sample volume within the centrifuge actually contains a distribution of gas densities. The lower pressure, longer lived fluorescence part will dominate the signal at late times. (Note: The software will record and store all data, but will use only data < 3 lifetimes in the least squares fit to determine intensity and lifetime.)

3) No more than 14 samples may be recorded per optical channel. This is a software array constraint and is not inherent in the system.

Operating Range

The temperature range for the system is limited by the available data base. The equations given for the temperature dependence of fluorescence lifetime and excitation cross section are valid only in the range 20^{o} - 60^{o}C.

Figure 15 shows the data from the 16th optical channel (of the 26 available channels) taken in the 12th run on October 3, 1984. The data were taken in the Los Alamos centrifuge (STR) and represent an accumulation of 200 laser pulses. The data show that

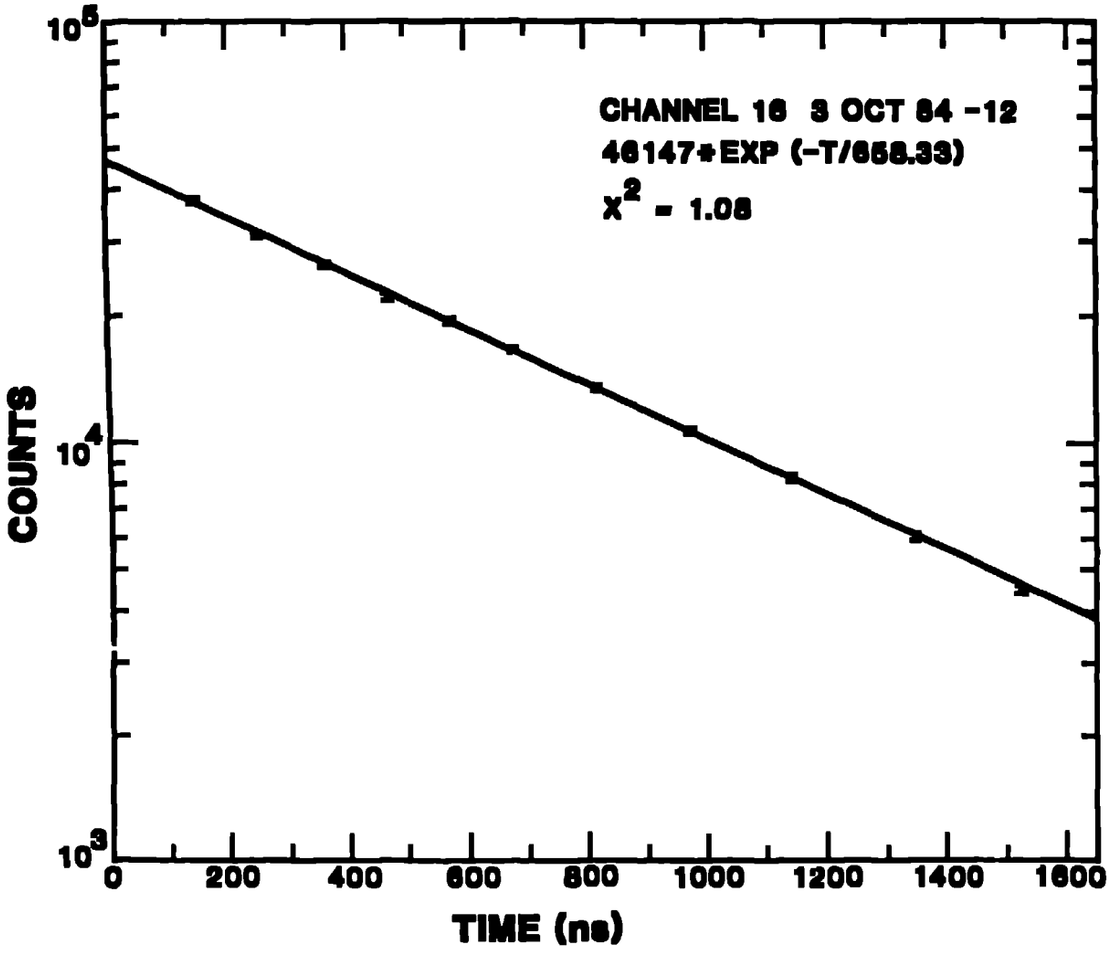

Fig. 15. Mid range data, 1.8 torr. The fluorescence signal from optical channel 16 was divided into 11 sampling regions. The vertical extent of the plotting symbols represent the average and standard deviations for each data point as determined during the 200 laser pulses used to accumulate these data.

the gas sample was at a pressure of 1.8 torr and 44°C, which is in the middle of the useful range of the LIF system.

Figure 16 demonstrates the high pressure limit of the system due to the constraint that all sampling must be done between 100 ns and 3 decay times after the laser pulse. The gas sample was at a pressure of 47.3 torr with a temperature of 49°C.

The signal strength decreases as pressure decreases because the number of initially excited molecules is proportional to molecular number density. However, the fluorescence efficiency increases with lifetime.

$$N_0^* \quad \text{is proportional to} \quad n \quad , \tag{6}$$

where,

$$N = \int_0^\infty N_0^* e^{-t/\tau} d\tau = N_0^* \tau \quad , \tag{7}$$

n = molecular number density ,

N_0^* = number of initially excited molecules ,

and

N = number of fluorescence photons .

The result of these two relationships is that the detected number of photons will fall only a factor of 15 when the pressure is reduced from 100 to 0.01 torr. The number of counts/integrator decreases slowly with pressure as the gate widths increase from 20 to 200 ns.

Below a pressure of $\sim 1\frac{1}{2}$ torr (all gate widths are 200 ns and can no longer be widened in proportion to τ), the number of counts

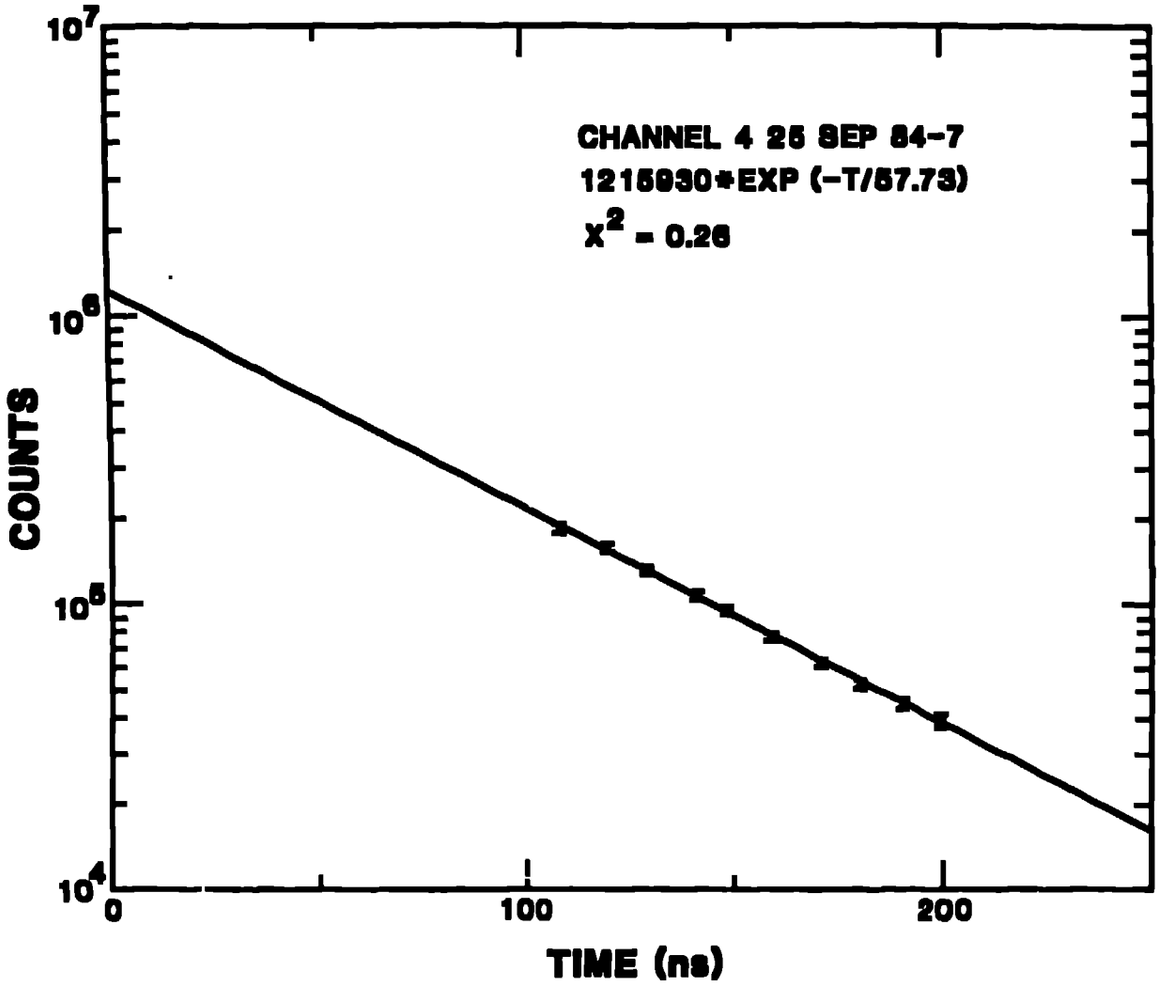

Fig. 16. High pressure limit, 47.3 torr. The requirement to record all data between 100 ns and three decay lifetimes after the laser pulse results in the high pressure limit of about 50 torr. In this "tail wagging the dog" extreme, a small error in slope leads to a large error in intensity. The X plotting symbol means that this point was not used in the least squares fit because it fell outside the three lifetime limit. These data were recorded using 50 laser pulses.

per integrator will decrease proportionally with pressure. (Note: the sensitivity of the photomultiplier/current integrator system is ~ 1 count/photon, so the signal strength can only be improved by increasing the laser power.) Figure 17 shows data taken near the low pressure limit. This data was taken with a gas pressure of 0.24 torr and is the sum of 50 laser pulses. Due to problems with optics inside the centrifuge, the laser power delivered to the gas is estimated to be only 100 μJ/pulse. (The laser can produce 5 mJ/pulse.) This implies that the low pressure limit for the system should be ~ 0.02 torr. Accurate initial intensity measurements can probably be made at 0.02 torr but gas diffusion and centrifuge rotation may limit the time span over which lifetime measurements can be made.

RESULTS

The entire LIF system was tested in the Los Alamos scoop test rig during September and October, 1984. These runs were used to 1) check reproducibility; 2) determine absolute and relative accuracies for both temperature and pressure; and 3) explore the limitations of the system. The rotational speed of the centrifuge was held constant during these runs, but the gas inventory and scoop radial position were varied.

Nineteen photomultiplier tubes were available for these runs. They were installed in optical channels 3 through 23 excluding channels 17 and 21. Channel 3 corresponded to the centrifuge wall location at speed, and channels 4 through 23 move away from the

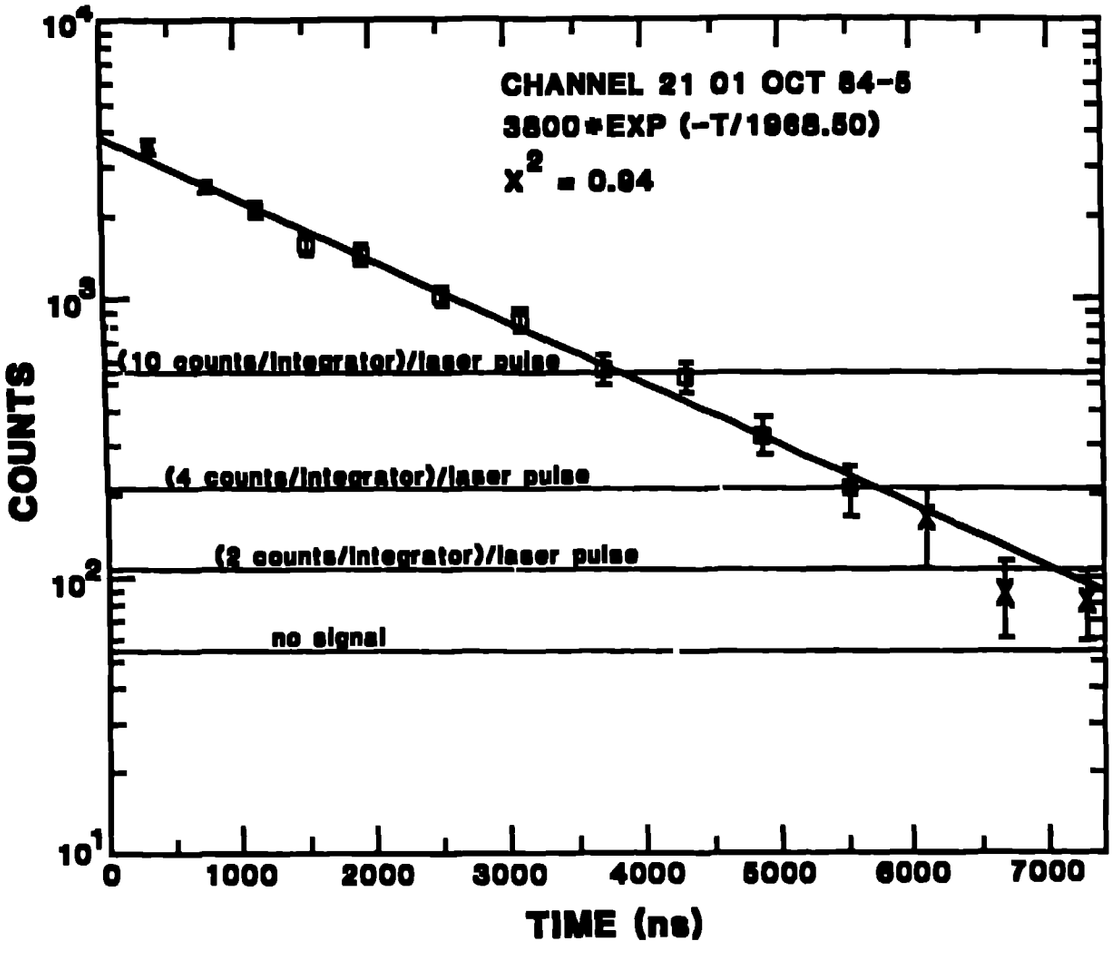

Fig. 17. Low pressure limit, 0.24 torr. This limit is due to low signal strength caused by low laser power. A more fundamental limit will result from gas diffusion and/or centrifuge rotation. These data were recorded using 50 laser pulses. Note, the position of the "(counts/integrator)/laser pulse" lines are the result of several calibrations and normalizations, and will vary with each data set.

wall (smaller radius). The number of available integrators (120 samples) limited to ten the number of channels which could be recorded simultaneously. Nineteen optical channels were recorded in two runs, one recording channels 3, 5, 7, 9, 11, 13, 15, 18, 19, 21 and the other recording channels 4, 6, 8, 10, 12, 14, 16, 18, 20, 23. The two runs could be made within four minutes with the actual sample time for each run being 5 - 20 seconds depending on the number of laser pulses used (10 Hz pulse rate). Channel 18 was used for intensity normalization.

Throughout this paper, locations will be given in terms of a scaled distance X:

$$X(r) = \frac{\omega^2 a^2}{2RT}\left(\frac{a^2 - r^2}{a^2}\right) \qquad (8)$$

where ω = angular velocity
a = centrifuge radius
R = gas constant
T = temperature

Reproducibility

Standard deviations for intensity and lifetime were determined by recording ten sets of data under identical running conditions. Each set contained data from ten optical channels ranging in lifetime from 103 to 1120 ns. Ten sets of data were recorded using 50 laser pulses per set and ten more sets were recorded using 200 laser pulses per set. The results are shown in Table 2.

TABLE 2

Optical Channel	Location X	Lifetime (ns)	Standard Deviation			
			50 laser pulses		200 laser pulses	
			Lifetime	Intensity	Lifetime	Intensity
4	.215	103.70	3.0%	6.0%	1.4%	4.6%
6	.641	137.07	3.3%	4.8%	0.9%	1.1%
8	1.07	187.66	1.3%	2.0%	0.9%	1.7%
10	1.49	262.24	2.3%	2.7%	0.6%	2.3%
12	1.91	317.77	0.9%	1.6%	0.5%	0.8%
14	2.33	402.92	2.8%	2.0%	2.5%	2.8%
16	2.74	638.95	2.2%	1.6%	1.0%	1.2%
18	3.15	749.00	1.4%	2.9%	0.7%	1.7%
20	3.55	911.85	1.8%	2.2%	1.2%	1.7%
23	4.16	1170.04	4.0%	3.5%	2.2%	1.8%

Pressure Extremes

Intensity and lifetime data were taken for three gas inventories under "wheel flow" conditions, i.e. no impediments to gas flow. Pressure and temperature profiles were computed for each gas inventory. The intent was that the high pressure end of the high gas inventory, and the low pressure end of the low gas inventory would be beyond the useful range of the measurement system.

Figure 18 shows the pressure profiles. The data are the intensity data normalized to the wall pressure (X = 0). The

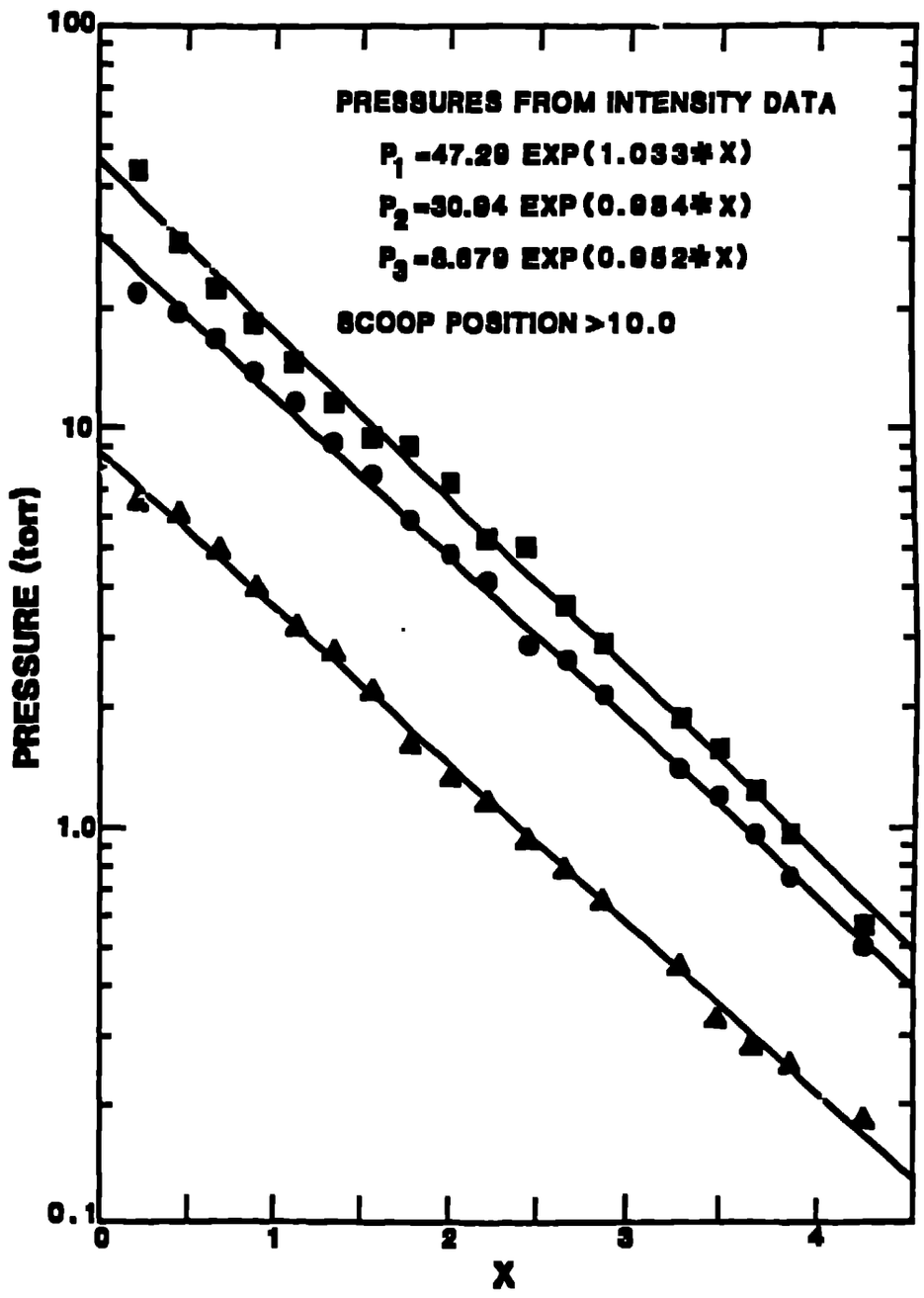

Fig. 18. Pressure profiles for three gas inventories under "wheel flow" conditions. The solid lines are least squares fits of the data.

intensity data from channel 3 (X = 0) are not valid because the centrifuge wall intercepts the volume of the channel. The radiating gas volume and therefore the apparent intensity are reduced. However, lifetime data are valid from this channel. The wall pressure is determined by assuming that the gas next to the wall surface is at the same temperature as the outside wall temperature (known via other means) and the use of Eq. 1. Note that the intensity data look very good down to the lowest pressure recorded (0.2 torr).

The solid lines shown in Fig. 18 are least squares fits of the data. A quality of the fit can be defined

$$\sigma = \left| \frac{1}{18} \sum_{i=1}^{18} \left(\frac{\text{Data}_i - \text{Fit}_i}{\text{Fit}_i} \right)^2 \right|^{1/2} \qquad (9)$$

For these three data sets

$\sigma_1 = 0.082$ (high wall pressure - 75 laser pulses)

$\sigma_2 = 0.052$ (medium wall pressure - 100 laser pulses)

$\sigma_3 = 0.050$ (low wall pressure - 50 laser pulses)

About $\frac{1}{2}$ the average error is due to channel 4 (X = 0.0068). This channel's proximity to the wall makes it vulnerable to reflections and/or fluorescence from wall materials. Even discounting channel 4, deviations from the fit are greater than those predicted by Table 2.

Run	Measured σ (Fig. 18)	Predicted σ (Table 2)
1	4.6%	2.2%
2	2.2%	2.2%
3	4.2%	2.8%

The above table, although a small statistical sample, would indicate that there exists a relative, channel to channel error of ~ 1% which cannot be improved through photon statistics (more total laser energy). Note: This analysis assumes that the true pressure profile really is exponential.

Figure 19 shows the temperature profiles corresponding to Fig. 18. The temperatures were calculated by using pressures, as determined from the least squares fit (Fig. 18), and the measured lifetime from each channel to solve Eq. 1. The continuous lines through the data are "eyeball" fits meant only to guide the eye. Wheel flow theory assumes a constant temperature throughout the gas, an assumption not supported by the data.

The three temperature profiles of Fig. 19 can generally be described as flat near the wall, then rising more rapidly as pressure decreases. The rise becomes particularly rapid below 1 torr. Three explanations come to mind concerning this unexpected temperature rise:

1) The profiles are correct;

2) The system biases long lifetime data;

3) Equation 1 is incorrect.

An artificially high temperature would be calculated if the calculated pressure were low, or the measured fluorescence decay time were short. The pressure profiles are shown in Fig. 18 and agree with theory. Two physical processes could shorten the measured lifetime. First, excited molecules can diffuse out of

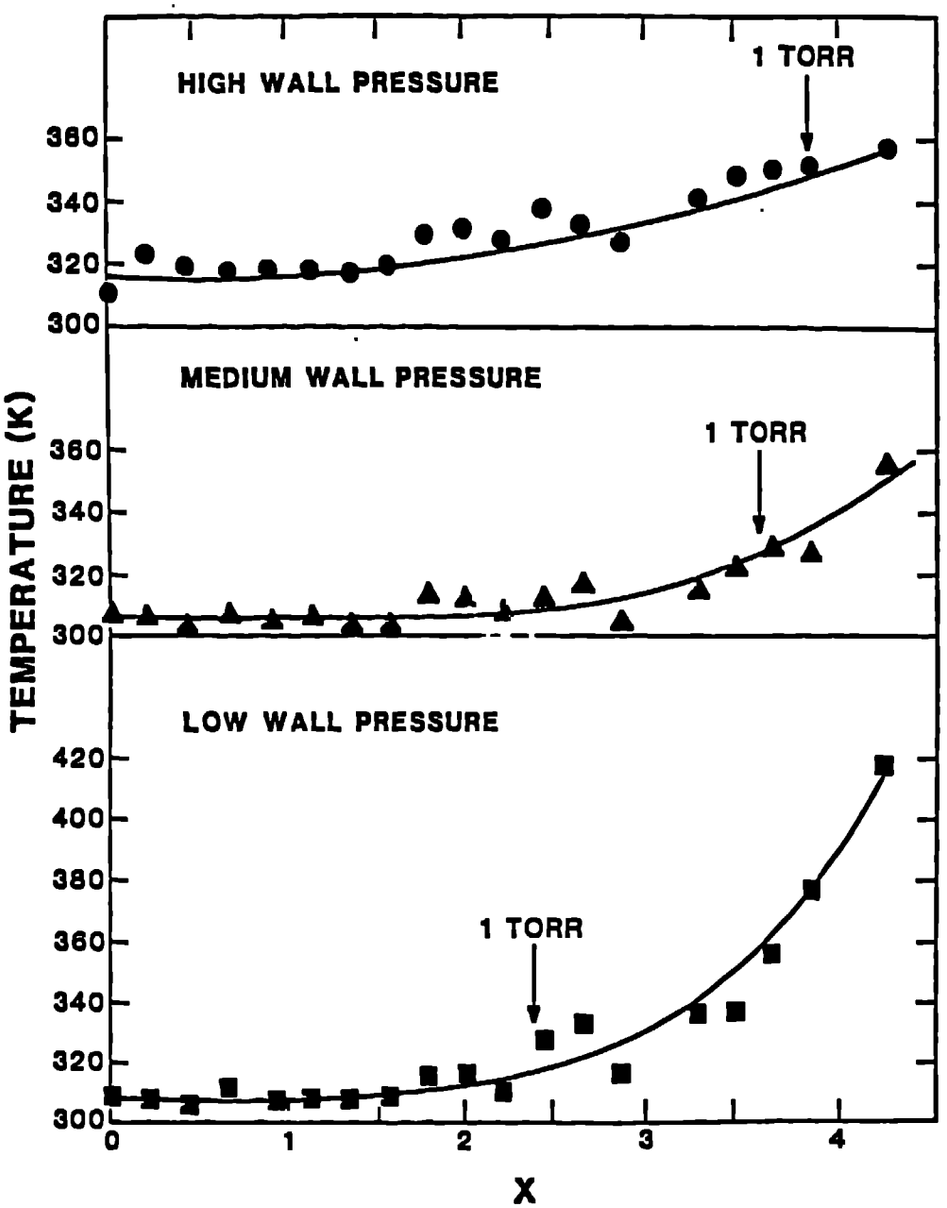

Fig. 19. Temperature profiles for three gas inventories underheel "wheel flow" conditions. The solid lines through the data are meant only to guide the eye.

the observed radial zone. (This is not important for pressures above ~ 0.05 torr.) Second, the recorded intensity will decrease due to the effects of geometric optics as the gas rotates away from the telescope axis. (This effect could change the lifetime of the lowest pressure recorded from 1770 ns to 1812 ns which lowers the calculated temperature from 419°K to 415°K.) Finally, Figs. 20, 21, 22 are offered as testimony to the quality of the lifetime data. These are the low pressure extremes for the three runs discussed in this section.

Fig. 2 shows some of the data base for Eq. 1. The equation fits the data very well, but two observations must be made: First, the temperature range is only 20° - 60°C (293 - 333°K) and no claim to validity outside this range is made. Secondly, Eq. 1 uses twelve parameters. A glance at these parameters and their error bars as listed in Table 1 would indicate that the convergence of these parameters to their central values is not very strong. Perhaps a different, but equally consistent, set of parameters would change the temperature profiles of Fig. 19.

Effect of Scoop Location

Using the medium wall pressure inventory of the previous section, lifetime and intensity data were recorded while the scoop was adjusted to five radial locations. The scoop was displaced axially several inches from the LIF observation region.

Table 3 and Fig. 23 describe the pressure profiles as a function of scoop location. The trend is toward a steeper profile as the scoop is pushed further into the gas.

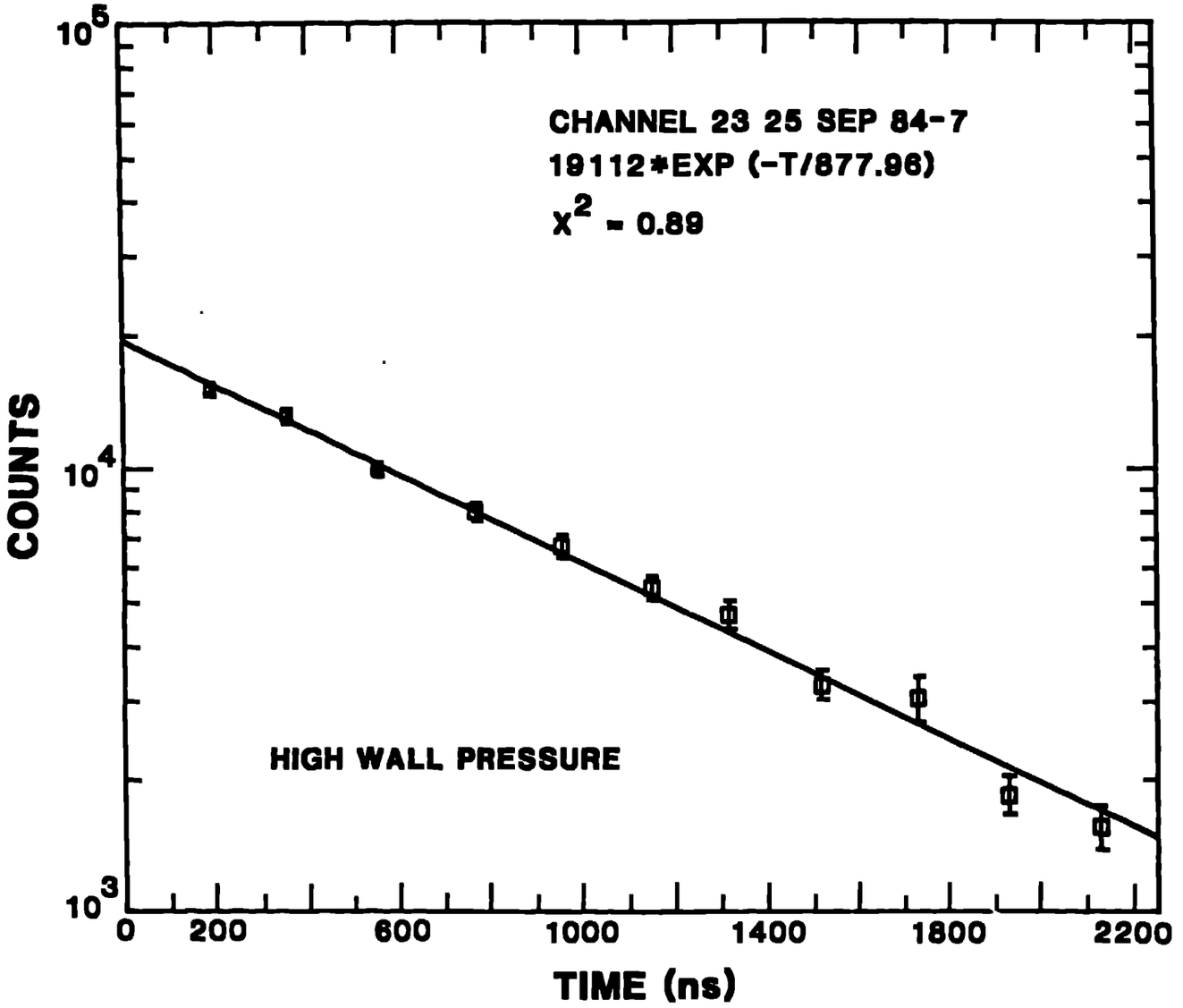

Fig. 20. Low pressure fluorescence decay for high gas inventory. Pressure equal to 0.65 torr.

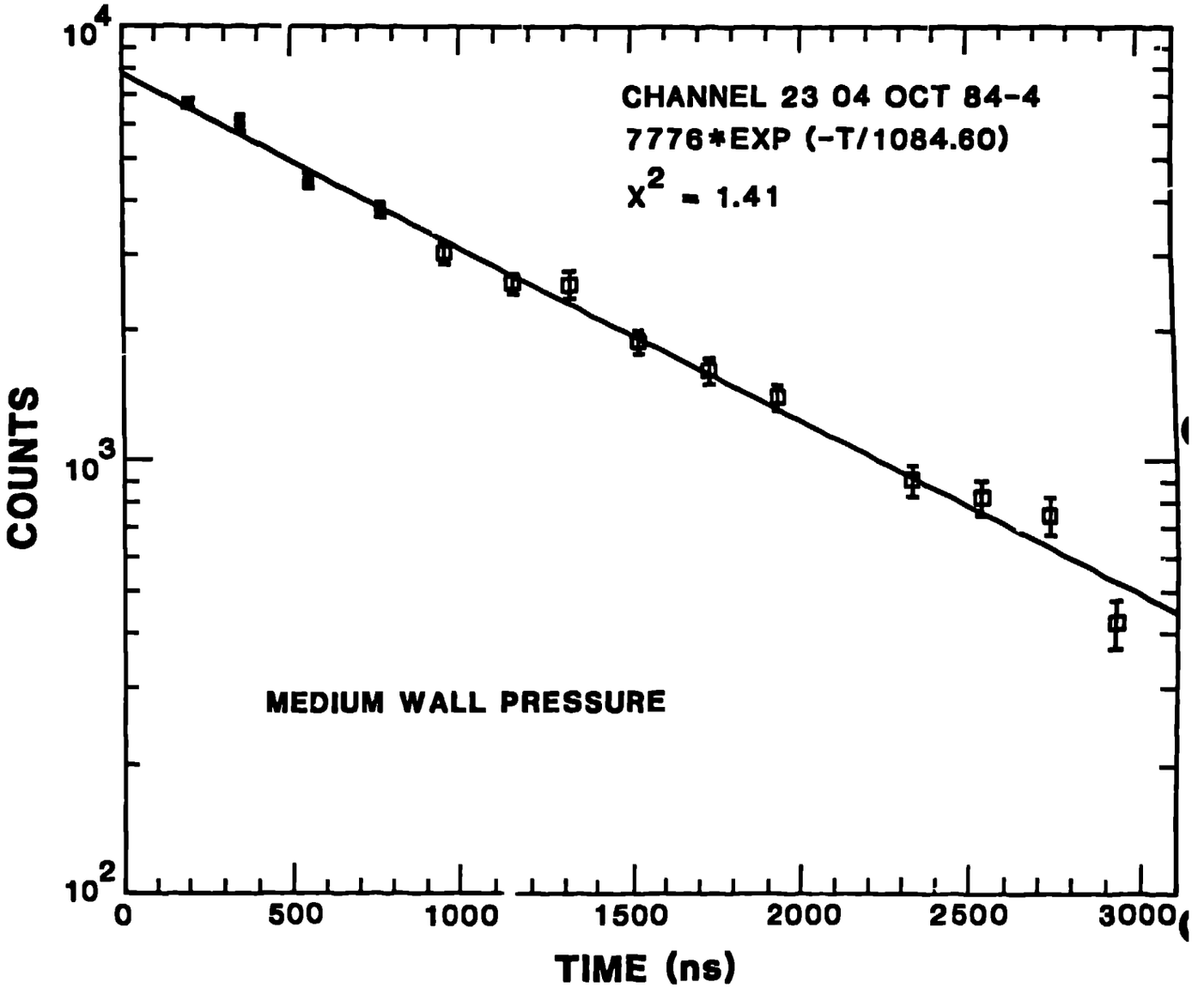

Fig. 21. Low pressure fluorescence decay for medium gas inventory. Pressure equal to 0.50 torr.

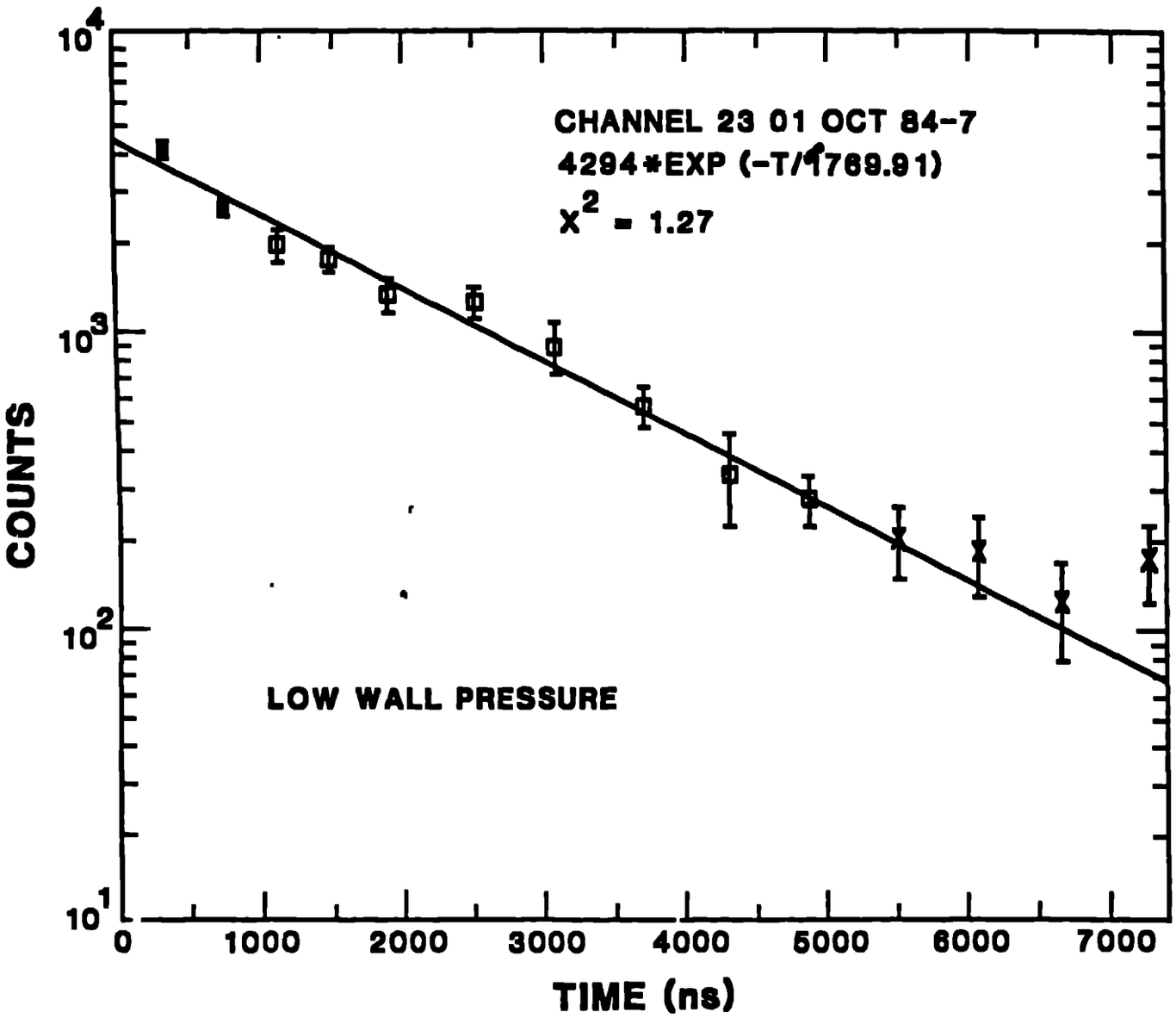

Fig. 22. Low pressure fluorescence decay for low gas inventory. Pressure equal to 0.17 torr.

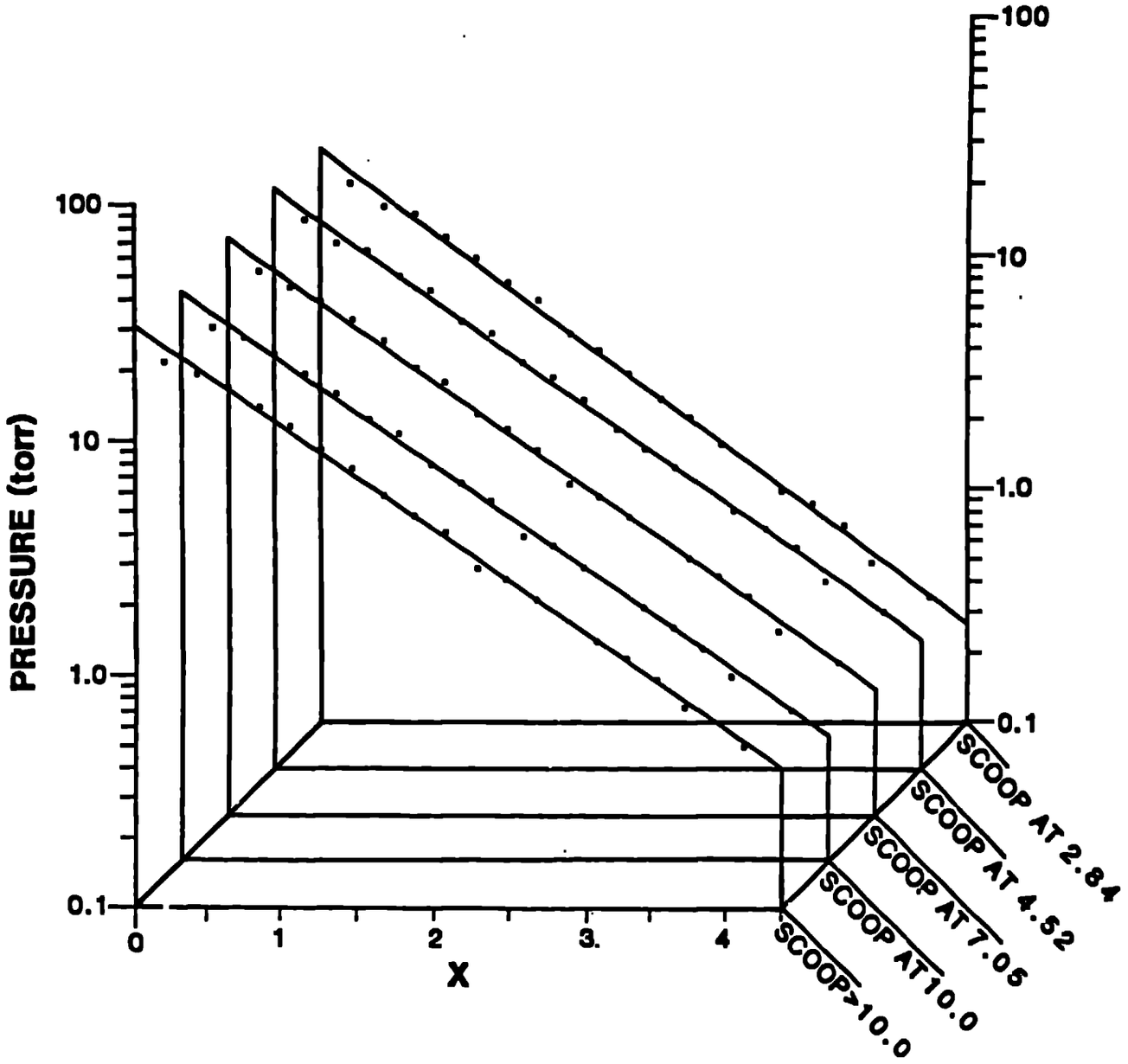

Fig. 23. Pressure profiles for medium gas inventory at five gas scoop locations. The lines through the data are exponential least squares fits (see Table 3).

TABLE 3

Scoop Location	Fit (18 channels)	σ
> 10.0	30.94 exp (.984 *X)	5.23%
10.0	27.20 exp (.989 *X)	5.42%
7.05	29.28 exp (1.00 *X)	5.34%
4.52	29.62 exp (.996 *X)	5.38%
2.84	27.61 exp (1.05 *X)	6.04%

The lead factor of the fit is the wall pressure (torr) as determined from an externally measured wall temperature and the fluorescence lifetime in channel 3. A comparison of these numbers is an indication of the absolute accuracy of the measurement. (The fifth line should be excluded because the gas loss rate was high during this run.) This would appear to be a worst case since these pressures are deduced from lifetime data recorded in channel 3 and subject to the wall effects of reflection and fluorescence, but the mean and standard deviation of the first four lines in Table 3 are 29.26 torr ± 5.3% which just happens to be the same accuracy as all the other pressures as determined via intensity data.

Figure 24 displays the temperature profiles for these runs. The overall gas temperature increases only gradually until the scoop is placed far out into the gas.

CONCLUSIONS

The data exhibited here indicate that the LIF system is capable of absolute pressure and temperature measurements to

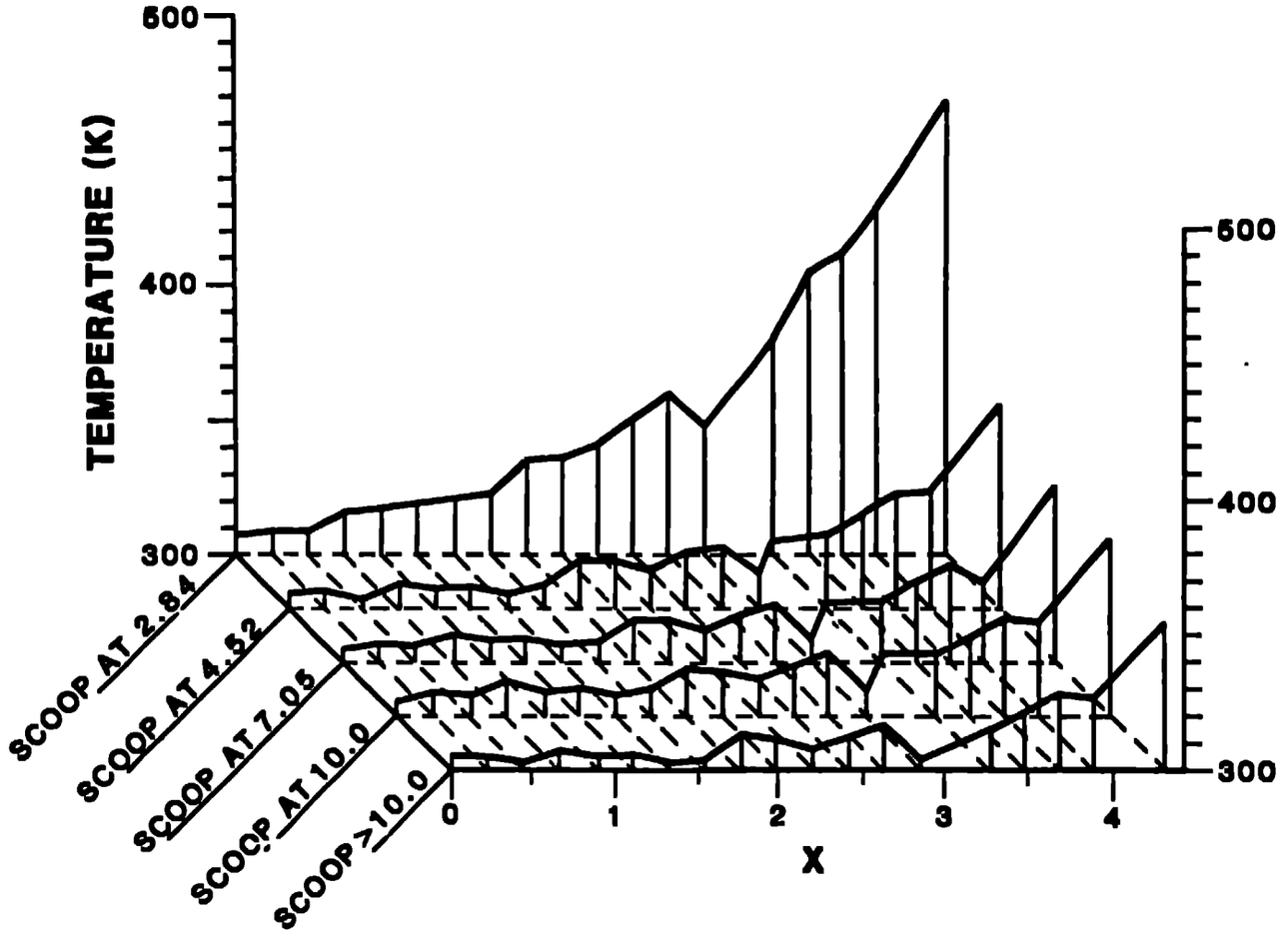

Fig. 24. Temperature profiles for medium gas inventory at five gas scoop locations.

within a few percent when data is summed over at least 50 laser pulses. At present the temperature determination is suspect because the data base on which Eq. 1 is founded needs to be expanded to include much higher temperatures. The useful pressure range is approximately 0.05 to 50 torr.

The analysis used in this work is not complete. Equation 4 shows that the excitation cross section, and therefore the fluorescence intensity, is temperature dependent. The pressure profiles should be corrected by including this temperature effect, which in turn, affects the temperature profiles. The iteration can be continued as needed. This procedure was not followed here because Eq. 4 is valid only in the temperature range 20° - 60°C. The empirical nature of this equation means that it cannot be used outside this range. Again, the useful range of this equation needs to be extended.

REFERENCES

1. S. DeSilvestri, O. Svelto, F. Zaraga, Appl. Phys. 21, 1 (1980).

2. O. DeWitte, R. Dumanchin, M. Mickon, and J. Chatelet, Chem. Phys. Lett. 48, 505 (1977).

3. F. B. Wampler, R. C. Oldenborg, and W. W. Rice, Chem. Phys. Lett. 54, 554 (1978).

4. R. C. Oldenborg, W. W. Rice, and F. B. Wampler, J. Chem. Phys. 69, 2181 (1978).

5. W. W. Rice, R. C. Oldenborg, P. J. Wantuck, J. J. Trice, and F. B. Wampler, J. Chem. Phys. 73, 3560 (1980).

6. F. B. Wampler, private communication.